Reducing Glucocorticoid Burden in Lupus with Omega-3 Fatty Acids: Docosahexaenoic Acid Augments Prednisone Efficacy in Maintaining Cyclophosphamide-Induced Remission of Preclinical Lupus Nephritis

Ashley N. Anderson[1], Olivia F. McDonald[1,2], Shayla-Rae Johnson[1], John J. Liddle[1], Vanessa Estrada[1,2], Jalen T. Jackson[1], Ryan P. Lewandowski[3], James G. Wagner[2,3], Jack R, Harkema[2,3,4], James J. Pestka[1,2,5.]

[1] Department of Microbiology, Genetics, and Immunology, Michigan State University, East Lansing, MI, United States; [2] Institute for Integrative Toxicology, Michigan State University, East Lansing, MI, United States; [3] Department of Pathobiology and Diagnostic Investigation, Michigan State University, East Lansing, MI, United States; [4] Department of Pharmacology and Toxicology, Michigan State University, East Lansing, MI, United States; [5] Department of Food Science and Human Nutrition, Michigan State University, East Lansing, MI, United States

Corresponding Author:

Dr. J.J. Pestka
Department of Microbiology, Genetics, and Immunology
Michigan State University
East Lansing, MI, United States
Email: pestka@msu.edu

Running Title: DHA Supplementation Augments Lupus Nephritis Remission

Keywords: NZBWF1 mouse, lupus nephritis, omega-3 fatty acid, prednisone, cyclophosphamide

Abstract

Background: Managing lupus nephritis (LN) remains challenging due to relapses after immunosuppressive induction and toxicity from long-term glucocorticoid (GC) maintenance therapy. Dietary omega-3 fatty acids prevent LN onset in preclinical models, but their role in maintaining remission post-induction remains unstudied.

Methods: The silica-accelerated LN (SALN) model using lupus-prone NZBWF1 mice was used to evaluate how docosahexaenoic acid (DHA), an omega-3 fatty acid, influenced LN remission durability after cyclophosphamide (CYC) induction, alone or with a modest dose of prednisone (PDN). Mice received intranasal silica weekly from 8 to 11 weeks. After LN developed at 21 weeks, groups were injected weekly with CYC (HED=31 mg/d) or vehicle (VEH) for 8 weeks, during which CYC groups also received control, DHA (HED=5 g/d), PDN (HED=9 mg/d), or DHA+PDN diets. Disease activity was monitored via proteinuria, autoantibodies, and survival. Six weeks post-CYC, multi-organ histopathology and immunohistochemistry were assessed.

Results: VEH-treated mice developed severe LN with early death. CYC slowed disease temporarily in control- and PDN-fed mice; relapses occurred after cessation. DHA or DHA+PDN increased tissue omega-3 levels and prolonged remission. PDN and DHA monotherapies and co-therapy improved survival, but DHA+PDN was most effective at sustaining remission as reflected by reduced histopathologic markers of lupus severity in the kidney, spleen, lung, and brain.

Conclusion: DHA+PDN optimally maintained LN remission after CYC, supporting omega-3 supplementation as a potential GC-sparing strategy to improve immunosuppressive therapy and prevent relapses.

Highlights

- Frequent post-immunosuppressive treatment flares and the toxicity from long-term maintenance therapy with glucocorticoids (GCs) limit effective management of lupus nephritis (LN).
- The silica-accelerated lupus nephritis (SALN) model in NZBWF1 mice mimics the gene–environment interactions of human SLE and LN, enabling synchronized and efficient preclinical studies of drug and nutritional interventions.
- Short-term immunosuppressive therapy with cyclophosphamide (CYC) induces temporary remission of LN and extrarenal inflammation and autoimmunity in SALN mice, which can be extended through monotherapy with either dietary supplementation with omega-3 docosahexaenoic acid (DHA) or a moderate dose of the GC prednisone (PDN).
- Combining maintenance therapy with DHA and PDN proved more effective than monotherapy in enhancing the durability of post-CYC LN remission and in reducing extrarenal inflammation and autoimmunity in the lung, spleen, and brain.
- These preclinical findings show that dietary supplementation with omega-3s such as DHA may offer a safe, affordable, GC-sparing adjunctive option for managing LN and SLE.

Introduction

Systemic lupus erythematosus (SLE) is a severe, multifactorial autoimmune disease that causes immune-mediated damage across multiple organs, including the skin, spleen, lungs, brain, and kidneys [1-4]. Its onset and progression are driven by complex gene–environment interactions and characterized by recurrent flares that substantially increase morbidity and the risk of irreversible organ damage. Lupus nephritis (LN) is a major complication that can progress to end-stage renal disease when inadequately controlled [1,4,5].

Conventional therapy for advanced proliferative LN (Class III or higher) typically follows a two-phase paradigm to quell renal inflammation, suppress autoimmunity, and promote durable remission [6]. The induction phase uses potent immunosuppressants such as cyclophosphamide (CYC) to achieve LN remission, followed by a maintenance phase to sustain remission and limit cumulative damage, using tapered doses of glucocorticoids (GCs) like prednisone (PDN) together with other drugs, such as mycophenolate mofetil [7,8]. Although these regimens are effective, GCs have myriad adverse effects—including serious infections, fatigue, metabolic and cardiovascular complications, type 2 diabetes, bone loss, reproductive and hepatic toxicity, and bone marrow suppression—that pose ongoing challenges in selecting drugs, determining treatment duration, and designing tapering strategies. Importantly, prematurely reducing or stopping maintenance therapy significantly increases the risk of relapse and flaring [9]. Recent advances in biologic and targeted therapies have expanded the LN armamentarium and can theoretically reduce GC exposure [6], yet their high cost and restricted availability remain significant barriers for the ever-growing population of patients without adequate insurance coverage [10].

There is increasing recognition that dietary modulation has value as a complementary strategy for

82 treating persistent inflammatory and autoimmune diseases, an emphasis reflected in initiatives such
83 as the NIH Strategic Blueprint on Precision Nutrition and the NIH-Wide Strategic Plan for
84 Autoimmune Disease Research [11,12]. Consistent with this recognition, many clinicians are
85 adopting dietary counseling into routine SLE care [13], and there is particular interest in precision
86 nutrition approaches that target the tissue lipidome by increasing consumption of omega-3
87 polyunsaturated fatty acids (PUFAs) [14-16]. Western dietary patterns, typically enriched in omega-
88 6 PUFAs such as linoleic acid (LA) from seed oils and arachidonic acid (ARA), formed by LA
89 elongation and found in animal fat, are associated with worsening of chronic inflammatory states
90 driven by ARA-derived metabolites [17]. In contrast, diets or supplements rich in marine-derived
91 omega-3 PUFAs—especially docosahexaenoic acid (DHA) and eicosapentaenoic acid (EPA),
92 sourced from microalgae, krill, or cold-water fish oils—can attenuate inflammatory responses and
93 promote their resolution [18].

94 A well-established literature links DHA and EPA intake of 1 to 5 g/day to favorable changes in
95 cardiovascular risk biomarkers and outcomes, as well as clinical improvement in inflammatory
96 rheumatologic conditions [19-23]. Regulatory investigations confirm that combined EPA+DHA
97 supplementation up to 5 g/day is safe for adults [24]. This dosage costs approximately $2/day when
98 purchased over the counter as a stable, high-quality supplement [25]. Mechanistically, omega-3s are
99 rapidly incorporated into immune cell membranes and act by i) altering membrane fluidity and lipid
100 raft organization to modulate receptor clustering and downstream signaling, ii) dampening
101 activation of proinflammatory transcription factors such as NF-κB while activating others with anti-
102 inflammatory actions like PPAR-γ, iii) reducing proinflammatory gene expression and cytokine
103 production, iv) suppressing production of inflammatory ARA-derived leukotrienes, prostaglandins,
104 and thromboxanes by competitive inhibition, and v) serving as substrates for specialized pro-

105 resolving mediators that drive active resolution of inflammation and restoration of tissue
106 homeostasis [15,18,26]. Remarkably, many of these molecular targets overlap with or complement
107 those of GCs [27], offering promise of safe adjunctive omega-3 supplementation to reduce flare
108 frequency and slow kidney damage in individuals with lupus.

109 Preclinical investigations in lupus-prone mouse strains over four decades have consistently shown
110 that omega-3-enriched diets suppress or delay autoimmune responses, reduce the onset and
111 progression of LN, and improve survival rates [28-53]. In contrast, diets high in saturated fats,
112 monounsaturated fats, and omega-6s, typical of ultraprocessed foods, have been linked to increased
113 autoimmunity and kidney damage. Building upon this base, our lab has developed an efficient gene–
114 environment interaction model in autoimmune-prone NZBWF1 mice, in which short-term, repeated
115 intranasal instillations of crystalline silica ($cSiO_2$), a well-known environmental trigger of lupus,
116 accelerate systemic autoimmunity and LN by approximately three months, providing a highly
117 reproducible silica-accelerated LN (SALN) platform [54,55]. Within this model, oral
118 supplementation with microalgal oil–derived DHA at human-equivalent doses (HEDs) of 2 to 5
119 g/day provides broad dose-dependent protection, including: i) suppression of inflammatory, type I
120 interferon, and autoimmune gene networks in the lung; ii) reduction of B- and T-cell infiltration and
121 ectopic lymphoid structure (ELS) formation; iii) lowering of pulmonary and systemic autoantibody
122 (AAb) titers; iv) prevention of glomerulonephritis; and v) prolonging survival [26,56-63].
123 Collectively, these studies position DHA supplementation as a suitable adjunctive strategy for
124 reducing GC use during LN treatment.

125 The SALN model has been further leveraged to assess the preventive effectiveness of the PDN,
126 demonstrating that oral pretreatment with a medium PDN dose (14 mg/day HED) substantially
127 reduced $cSiO_2$-induced pulmonary ELS formation, AAb production, and inflammatory and

128 autoimmune gene expression in the lung and kidney. This dose also reduced splenomegaly and the
129 severity of glomerulonephritis [64]. In contrast, low-dose PDN (5 mg/day HED) did not improve
130 autoimmune symptoms, whereas a high-dose PDN (46 mg/day HED) caused severe GC-associated
131 toxicity, leading to early cohort termination. Significantly, even at the effective medium dose, PDN
132 caused muscle wasting and did not improve survival. This indicates a discordance between
133 histopathologic improvements and death rates in SALN and confirms the narrow therapeutic
134 window of long-term GC therapy [64]. Furthermore, these observations suggest that, within the
135 constraints of the SALN model, DHA offers a more favorable balance between preventive
136 effectiveness and tolerability than PDN.

137 Although a substantial amount of preclinical data supports the use of omega-3s in lupus, including
138 research with DHA in SALN, these studies have primarily focused on preventing as opposed to
139 treating established disease. This limits their relevance for patients with SLE who often present with
140 active LN that requires remission induction. To address this gap, SALN was used here to assess
141 whether adjunctive DHA supplementation can maintain LN remission after immunosuppressive
142 induction with CYC, when administered either alone or combined with a moderate, clinically
143 relevant dose of PDN. We show for the first time preclinical evidence that adjunctive DHA improves
144 the efficacy of PDN, prolonging remission of both LN and extrarenal lupus pathogenesis.
145 Accordingly, safe, inexpensive omega-3 supplementation might serve as a GC-sparing strategy to
146 improve long-term disease management and reduce treatment-related toxicity in LN and SLE.

147 Materials and Methods

148 Animals

149 All experimental protocols were reviewed and approved by the Institutional Animal Care and Use

150 Committee (IACUC) at Michigan State University in accordance with the NIH guidelines (AUF
151 #PROTO202400258). Female 7-week-old lupus-prone NZBWF1 mice were obtained from the
152 Jackson Laboratory (#100008, Bar Harbor, ME), randomly assigned four per cage with free access
153 to food and water, and kept at a consistent temperature (20–24 °C) and humidity (30–70%) with a
154 12-hour light/dark cycle.

155 **Diets**

156 Diet formulations were based on the nutritionally balanced semi-purified American Institute of
157 Nutrition (AIN)-93G rodent diet containing 70 g soybean oil per kg of diet (AIN-93G rodent diet
158 #110700, Dyets Inc., Bethlehem, PA) [65] (Supplemental Table 1). Four experimental diets were
159 used in the study (Table 1). The (i) basal control diet (CON) was made by replacing the 70 g/kg
160 soybean oil with 60 g/kg of high-oleic safflower oil (AVO high-oleic safflower oil, American
161 Vegetable Oils, Inc., Commerce, CA) and 10 g/kg of corn oil (Mazola Corn Oil, ACH Food
162 Companies, Inc., Oakbrook Terrace, IL) to supply essential fatty acids. For the (ii) DHA diet, 25
163 g/kg of high-oleic safflower oil was substituted in the basal CON diet with 25 g/kg of microalgal oil
164 containing 40% DHA (DHASCO, DSM Nutritional Products, Columbia, MD), as described earlier
165 [56,57]. This diet contained 10 g/kg DHA, modeling human DHA intake of 5 g per day on a caloric
166 basis (Table 1). For a patient, this would be roughly equivalent to taking i) five triple-strength over-
167 the-counter fish oil capsules daily, each containing approximately 1 g of omega-3 fatty acids or ii)
168 five prescription-grade omega-3 capsules used to treat hypertriglyceridemia. For the (iii) PDN diet
169 and the (iv) combined DHA+PDN diet, PDN was dissolved in a small amount of 100% (v/v) ethanol
170 and added to both the basal CON and DHA diets at 10 mg/kg, as previously described [64]. This
171 dietary level corresponds to an HED of 9.4 mg/day (Table 2) and was designated as "moderate"
172 because it falls within the lower end of the medium dose range (7.5 to 30 mg/d) used in GC treatment

173 of rheumatic diseases [66].

174 **Crystalline silica ($cSiO_2$)**

175 $cSiO_2$ (Min-U-Sil-5, 1.5–2.0 μm average particle size, U.S. Silica, Katy, TX) was acid-washed in
176 1 M HCl at 100°C for 1 hour to remove surface contaminants that could obscure surface activity.
177 The $cSiO_2$ was then rinsed three times with sterile water and dried in an oven at 200°C to eliminate
178 water, endotoxins, and microbial contaminants. On each day of $cSiO_2$ instillation, a working stock
179 suspension of 40 mg/ml in Dulbecco's phosphate-buffered saline (DPBS) was prepared, then
180 sonicated for 1 minute using the Q125 Qsonica sonicator (Qsonica LLC, Newtown, CT) set to 2
181 minutes with pulses of 5 seconds on and 5 seconds off at 35% amplitude. After sonication, the
182 suspension was inverted and vortexed continuously during instillations to prevent $cSiO_2$ settling.

183 **Experimental design**

184 The experimental study design is depicted in Figure 1. NZBWF1 mice (7 weeks old) were started
185 on the CON diet, and one week later, they were anesthetized with 4% isoflurane and intranasally
186 instilled with 1.0 mg of $cSiO_2$ in 25 μl of DPBS once a week for 4 weeks [54]. The total $cSiO_2$ dose
187 (4 mg) approximately equals half of a human lifetime exposure according to guidelines set by the
188 Occupational Safety and Health Administration (OSHA)[67]. At 20 weeks of age, $cSiO_2$-treated
189 mice were divided into weight-based quartiles, with 1 mouse from each quartile housed together,
190 totaling 4 mice per cage. This grouping ensured balanced experimental conditions, reducing
191 confounding effects from body weight differences. At 21 weeks, when $cSiO_2$-treated mice exhibit
192 proteinuria (Supplemental Figure 1), cages were split into five treatment groups: (i) weekly DPBS
193 vehicle (VEH) intraperitoneal (IP) injections with the CON diet ($cSiO_2$/VEH/CON), (ii) weekly
194 CYC IP injections at 35 mg/kg body weight (bw) with the CON diet ($cSiO_2$/CYC/CON), (iii) weekly

195 CYC IP injections with a DHA diet ($cSiO_2$/CYC/DHA), (iv) weekly CYC IP injections with a PDN
196 diet ($cSiO_2$/CYC/PDN), and (v) weekly CYC IP injections with a DHA+PDN diet
197 ($cSiO_2$/CYC/DHA+PDN) (Figure 1). To reduce lipid oxidation products, diets were prepared every
198 two weeks, stored at -20°C until used, and provided fresh to the mice daily. Injections with VEH or
199 CYC ceased after 8 weeks, but mice remained on their respective maintenance diets for the
200 remainder of the study. Urine was collected weekly and tested for protein using reagent dipsticks
201 (Siemens Uristix 4, Malvern, PA). Plasma samples were collected biweekly, starting at 27 weeks of
202 age, for blood urea nitrogen (BUN) and AAb analyses. Mice were monitored daily for clinical signs
203 of moribundity (Supplementary Table 2) during feedings, and their body weights were recorded
204 weekly. Any mice meeting moribund criteria were immediately euthanized and necropsied. The
205 study concluded at age 35 weeks with a full necropsy of all remaining animals.

206 **Necropsy and tissue selection for light microscopy**

207 Mice were anesthetized at the end of the study with IP injections at 250 mg/kg bw of sodium
208 pentobarbital. A midline laparotomy was performed, and approximately 0.8 ml of blood was drawn
209 from the inferior vena cava and collected in heparinized tubes (MiniCollect Capillary Blood
210 Collection Tube #450477, Greiner Bio-One, Monroe, NC). Animals were euthanized by
211 exsanguination through the inferior vena cava. After death, the trachea was exposed, cannulated,
212 and the heart and lungs were excised en bloc. A volume of 0.7 ml sterile saline was instilled via the
213 tracheal cannula and then withdrawn to recover bronchoalveolar lavage fluid (BALF). A second
214 intratracheal saline lavage was performed, and the collected BALF was combined with the first
215 sample. Organs selected for light microscopy and digital image analysis were harvested at necropsy
216 and fixed in 10% neutral buffered formalin for at least 48 hours. The left kidney, spleen, and brain
217 were fixed by immersion, while the left lung lobe was fixed by fluid inflation via the trachea at 30

218 cm gravitational pressure as previously described [57].

219 After fixation, cross-sectional (transverse/coronal) tissue blocks were cut from the left kidney (1-2
220 blocks covering the entire organ), left lung lobe (4 blocks covering the entire lobe), spleen (2 mid-
221 blocks from the body of the organ), and brain (1 block with hippocampus, at the level of the inner
222 ear). Tissue blocks were paraffin-embedded and sectioned at 5 microns. Tissue sections were stained
223 histochemically with Hematoxylin and Eosin (H&E, all organs) or Periodic Acid Schiff (PAS,
224 kidney) and immunohistochemically stained for CD3+ and CD45R+ T and B lymphoid cells,
225 respectively (lung and kidney), IBA-1+ monocytes/macrophages (lung and kidney), and IBA-1+
226 microglia in the hippocampus (brain). Details for immunohistochemistry and specific antibodies are
227 provided in the Supplemental Materials.

228 **Quantitative and semi-quantitative image analysis of histopathology**

229 Digital images of histological sections were obtained with an Olympus VS200 slide scanner with
230 ASW software (V.3.2.1) at 20x magnification (Evident Scientific, Waltham, MA). Digitally scanned
231 images were viewed with Olympus OlyVIA software (V.2.8) and whole-slide image analyses were
232 conducted using QuPath image analysis software (V.0.5.1) [68]. Regions of interest (ROIs) were
233 annotated prior to each quantitative analysis (Lung, whole lung lobe sections; Kidney, renal cortex
234 in sections). Abundance of immunohistochemical stains (density of IBA-1+, CD3+, CD45R+) was
235 graphically expressed as the percent of ROI area. Thresholds were created to model staining
236 positivity per tissue type. Identical settings per stain were used to assess positivity among
237 experimental groups.

238 Semi-quantitative image analysis of histopathologic severity was conducted for specific lupus-
239 related lesions: membranous glomerulonephritis, renal tubular regeneration, accumulated protein in

240 renal tubular lumens, ectopic lymphoid structures (CD3+ T cells and CD45R+ B cells) in the kidney,
241 white pulp hyperplasia in the spleen, and microgliosis in the hippocampus of the brain (IBA-1+
242 microglia). A board-certified veterinary pathologist (JRH) examined all digitally scanned images of
243 routine H&E- and immunohistochemically stained tissue sections for $cSiO_2$-triggered lupus
244 histopathology using unbiased blinded assessment (no previous knowledge of individual animal
245 exposure or treatment). Lesion severity scores were recorded in a manner that is consistent with
246 state-of-the-art guidelines for semi-quantitative pathology assessment [69]. Criteria for ordinal
247 scoring were defined by percent of total tissue affected: 0 (no lesions) = 0% of total tissue; 1
248 (minimal) = less than 5%; 2 (mild) = 6 to 10%; 3 (moderate) = 11 to 50%; 4 (marked) = 51 to 75%;
249 5 (severe) = greater than 76%.

250 **Red blood cell (RBC) fatty acid analysis**

251 RBC fatty acid composition was analyzed using gas chromatography (GC) with flame ionization
252 detection by OmegaQuant Analytics (Sioux Falls, SD) as described previously [63]. Briefly, after
253 isolating RBCs from heparinized blood, fatty acid methyl esters (FAMEs) were prepared by heating
254 the RBCs with 14% boron trifluoride-ethanol and hexane at 100°C for 10 minutes. The FAMEs
255 were then extracted with hexane and analyzed on a Shimadzu GC-2010 chromatograph equipped
256 with an SP-2560 100-m capillary column. Fatty acids were identified by comparison to a
257 commercial standard (GLC OQ-A, NuCheck Prep). A total of 24 fatty acids were quantified and
258 expressed as a percentage of the total identified fatty acids, including saturated, monounsaturated
259 (cis and trans), and polyunsaturated (omega-3 and omega-6) species.

260 **Autoantibody (AAb) measurement**

261 IgG AAbs targeting silica-killed cell (SKC) autoantigens (AAgs) and dsDNA were measured using

262 an indirect ELISA based on a previously described method [70]. To prepare SKC AAgs, fetal liver-
263 derived alveolar-like macrophages (FLAMs) from lupus-prone NZBWF1 mice were exposed to 50
264 μg/ml $cSiO_2$ for 20 hours to induce cell death. The supernatant was then collected and stored at -
265 20°C until use. Poly-L-lysine-coated 96-well microplates were incubated with a blocking buffer
266 (PBS, 2% [w/v] BSA, 0.05% [v/v] Tween 20), then coated with 50 μl per well of either SKC AAg
267 diluted 1:20 or calf thymus dsDNA diluted to 2.5 μg/ml, both prepared in ELISA buffer (PBS, 0.1%
268 [w/v] BSA, 0.05% [v/v] Tween 20). Next, diluted BALF (1:1,000) or plasma (1:5,000 and 1:10,000)
269 was added to separate wells. A standard curve was generated using two-fold serial dilutions of a
270 mouse anti-dsDNA antibody, with the highest concentration assigned a value of 2,000 arbitrary units
271 (U). Bound AAbs were detected using HRP-conjugated goat anti-mouse IgG Fc antibody and K-
272 Blue® Advanced Plus TMB Substrate, with absorbance measured at 650 nm.

273 **Blood urea nitrogen (BUN) analysis**

274 BUN was measured using the Ray Biotech Urea Nitrogen Detection Assay Kit (MA-BUN-5) per
275 manufacturer's directions. Briefly, plasma samples were diluted 1:25, loaded onto a microplate, and
276 then incubated with an enzyme solution of urease and NADH. After a brief shaking of the plate,
277 absorbance was measured (340 nm) twice, with one minute between readings. The difference in
278 absorbance between the two readings correlates with BUN concentration. BUN levels were
279 determined using a standard curve.

280 **Bronchoalveolar lavage fluid (BALF) cell quantitation and identification**

281 Total cells in BALF were counted using a hemocytometer. Cytological slides were prepared by
282 centrifuging 150 μl of BALF for 10 minutes at 40× g, air-drying, and staining with the Easy III Step
283 Stain Kit (#ES902, Azer Scientific, Morgantown, PA). At least 150 cells were counted and

284 differentially identified as monocytes/macrophages, lymphocytes, or neutrophils based on
285 morphological criteria.

286 **Statistical analysis**

287 All treatment groups began with 8 mice. All statistical analyses were conducted using GraphPad
288 Prism 10 (V.10.6.1, Dotmatics, Boston, MA), with a p-value < 0.05 considered significant.
289 Parametric two-tailed t tests (with and without Welch's correction) or nonparametric Mann-Whitney
290 tests were used to compare the continuous quantitative data and the ordinal histopathological
291 severity scores between the $cSiO_2$/VEH/CON (negative control) and $cSiO_2$/CYC/CON (positive
292 control) groups, respectively. When comparing the continuous quantitative data across the treatment
293 groups ($cSiO_2$/CYC/CON, $cSiO_2$/CYC/DHA, $cSiO_2$/CYC/PDN, $cSiO_2$/CYC/DHA+PDN), several
294 statistical tests were performed: (i) parametric one-way ANOVAs along with the Brown-Forsythe
295 test of equal variances, (ii) parametric Brown-Forsythe and Welch one-way ANOVAs, and (iii)
296 Dunnett's and Tukey's multiple comparisons tests. When comparing the semi-quantitative ordinal
297 severity score data of the treatment groups, the nonparametric Kruskal-Wallis and Dunn's multiple
298 comparisons tests were used.

299

300 **Results**

301 **Dietary DHA remodels RBC membrane fatty acid composition**

302 The dietary DHA intervention was confirmed to induce systemic lipidomic changes by assessing
303 the fatty acid composition of RBC phospholipids, which serves as a biomarker of overall tissue lipid
304 status (Figure 2; Table 3) [71]. Mice receiving isocaloric DHA-supplemented diets

305 ($cSiO_2$/CYC/DHA and $cSiO_2$/CYC/DHA+PDN groups) exhibited significant increases (up to 10- to
306 12-fold) in DHA and other omega-3 fatty acids, including EPA and omega-3 docosapentaenoic acid
307 (DPA). This increase was accompanied by a marked decrease in total omega-6 fatty acids (up to 50
308 to 70%), such as arachidonic acid, omega-6 DPA, and docosatetraenoic acid, with the exception of
309 linoleic acid (LA), which was significantly elevated. Notably, RBCs from mice treated with DHA
310 and PDN contained higher levels of DHA, EPA, and total omega-3s than those from mice receiving
311 DHA alone, along with lower levels of ARA and total omega-6 fatty acids. In contrast, PDN
312 treatment alone did not alter fatty acid profiles, indicating that the observed lipidomic changes were
313 specifically attributable to dietary DHA intake.

314 **DHA and PDN co-therapy after CYC induction prevents proteinuria relapse and death.**

315 Consistent with previous studies in NZBWF1 mice [54,56,61], weekly intranasal $cSiO_2$ instillations
316 for 4 weeks in control-fed mice resulted in two main clinical outcomes: proteinuria (Figures 3A-C)
317 and shortened lifespan, with a median survival of 29.5 weeks (Figure 3D). CYC treatment alone
318 reduced proteinuria, but relapses happened after stopping, as evidenced by increased proteinuria at
319 week 33 (Figure 3A) , and increased median survival to 35 weeks (Figure 3D). Maintenance
320 therapies with either DHA or DHA+PDN delayed relapse, whereas PDN alone did not. The
321 percentage of proteinuric mice (Figure 3B) and mean proteinuria levels (Figure 3C) from weeks 21
322 to 35 were significantly lower in the CYC/DHA and CYC/DHA+PDN groups than in the CYC-only
323 or CYC/PDN groups. Maintenance treatments also conferred a survival advantage, with median
324 survival times for both monotherapies and combination therapy exceeding 35 weeks (Figure 3D).

325 **Combining DHA and PDN maintenance therapy preserves renal structure and reduces**
326 **macrophage infiltration.**

327 Kidneys from $cSiO_2$/VEH/CON mice exhibited severe membranous glomerular nephritis,
328 characterized by glomerular enlargement, extensive accumulation of Periodic acid Schiff (PAS)-
329 positive glomerular membranous tissue, and proteinaceous casts in the renal tubules (Figure 4B).
330 These features were absent in age-equivalent naïve mice from a prior study [61] and used here as a
331 standard reference control (Figure 4A). Conversely, CYC treatment reduced glomerulonephritis
332 (Figure 4C), and this improvement was further enhanced by DHA (Figure 4D) and PDN (Figure
333 4E). The group receiving combination therapy ($cSiO_2$/CYC/DHA+PDN) was the most protected
334 from these pathological changes and displayed nearly normal renal structure (Figure 4F). Semi-
335 quantitative scoring confirmed that the combination therapy decreased the LN severity score
336 ($p<0.01$) (Figure 4G), tubular protein score ($p=0.11$) (Figure 4H), and tubular regeneration score
337 ($p<0.05$) (Figure 4I) compared to CYC treatment alone.

338 IHC staining for IBA1, a well-known marker for recruited inflammatory monocytes/macrophages
339 [72], showed that, consistent with glomerulonephritis, $cSiO_2$ exposure caused significant infiltration
340 of monocytes/macrophages into interstitial spaces surrounding renal tubules and glomeruli in ELS
341 and some glomeruli (Figures 5A, 5B). While modestly reduced by CYC with DHA or PDN
342 monotherapies (Figures 5D, 5E, 5G), IBA1+ monocyte/macrophage infiltration was most robustly
343 reduced by co-therapy with CYC/DHA+PDN (Figures 5F, 5G). Accordingly, DHA+PDN co-
344 treatment was the most effective of the three maintenance therapies in reducing local renal
345 inflammation and preserving kidney structure.

346

347 **DHA and PDN co-therapy prevents the formation of renal ELS**

348 A key pathogenic feature of progressive LN is the formation of renal ELS [73-75]. The renal cortices

349 of $cSiO_2$-triggered mice that did not receive treatment contained large, organized ELS composed of
350 co-localized aggregations of $IBA1^+$ macrophages, $CD3^+$ T cells, and $CD45R^+$ B cells (Figure 6A, C,
351 E, G). Maintenance therapy with CYC/DHA+PDN effectively prevented this process, as kidneys
352 from this group were mostly free of dense lymphoid cell aggregate infiltrates and lacked organized
353 ELS architecture (Figure 6B, D, F, H). The kidney ELS score was lower ($p<0.01$) in the
354 CYC/DHA+PDN co-therapy group compared to the CYC-only control group, while DHA or PDN
355 monotherapies were less effective (Figure 6I).

356

357 **Protective effects of DHA and PDN monotherapy and co-therapy extend to the lungs.**

358 In NZBWF1 mice, age-related pulmonary perivascular and peribronchiolar lymphoid hyperplasia
359 spontaneously occurs at 8 to 12 months of age, during which polymorphic lymphoid infiltrates,
360 evocative of ELS, become dominated by CD4+ T cells, while B cells and antigen-presenting cells
361 segregate into a peripheral cuff surrounding the T cell–rich area [76,77]. This occurs much earlier
362 in the SALN model, where the lung is the hub for early cellular events that promote $cSiO_2$-induced
363 autoimmunity and the progression of lupus [78]. Cellular analysis of bronchoalveolar lavage (BAL)
364 fluid demonstrated that DHA and PDN monotherapies, as well as combination therapy with CYC,
365 reduced total inflammatory cells, monocytes/macrophages, and lymphocytes compared to CYC
366 alone (Figure 7A). Furthermore, combined DHA+PDN treatment exhibited a modest trend toward
367 reduced local production of IgG autoantibodies against dsDNA and $cSiO_2$-killed cells (Figure 7B).

368 Histological examination of lung tissue showed that, as previously reported [54,55], strong
369 perivascular ELS appeared in $cSiO_2$-treated mice (Figures 8C, D) and were absent in naïve mice
370 (Figures 8A, B). Consistent with decreased cellularity in BAL fluid, ELS were markedly reduced in

371 the lungs of the CYC/DHA+PDN group (Figures 8K, L), while effects of monotherapies were more
372 modest (Figures 8G-L). Semi-quantitative scoring confirmed that the DHA+PDN combination
373 maintenance therapy significantly lowered lung ELS scores ($p<0.001$) (Figure 9A), the percentage
374 of CD3+ T cells ($p<0.05$) (Figure 9C), and the percentage of C45R+ B cells ($p<0.0001$) (Figure
375 9D).

376

377 **PDN+DHA co-therapy suppresses $cSiO_2$-induced splenomegaly and systemic AAbs**

378 The spleen is another potential source of systemic AAbs in NZBWF1 mice [79], and splenomegaly,
379 a key feature of spontaneous lupus progression in these mice, is accelerated by $cSiO_2$ treatment [64].
380 Therefore, to evaluate the effects of treatments on systemic autoimmunity, we compared spleen
381 architecture and plasma AAbs across the experimental groups. $cSiO_2$ caused significant white pulp
382 hyperplasia in mice (Figures 10B, H), which was not evident in age-equivalent naïve NZBWF1 mice
383 (Figure 10A). Lymphoid cell hyperplasia was not substantially affected by CYC alone (Figure 10C)
384 or by CYC in combination with DHA or PDN alone (Figures 10D, E); however, it was suppressed
385 in CYC-treated mice that received PDN+DHA (Figure 10F). For other indicators of splenomegaly,
386 spleen weight and area, DHA and PDN monotherapies showed modest reductions, while
387 DHA+PDN co-therapy showed marked decreases (Figures 10G, H, and I). Treatment effects on the
388 spleen were consistent with plasma dsDNA and SKC AAb levels (Figure 10J). After stopping CYC,
389 plasma IgG AAbs against dsDNA and SKC began to rise again within 4 to 6 weeks post-CYC
390 treatment in the CYC-only and CYC/DHA groups. This increase was consistently suppressed in
391 groups receiving PDN, either alone or with DHA. Overall, DHA potentiates PDN suppression of
392 splenomegaly and systemic AAb formation resulting from $cSiO_2$ instillation.

393

394 **DHA and PDN co-therapy attenuates microglial cell activation in the brain**

395 NZBWF1 mice have been used in neuropsychiatric lupus (NPSLE) research, with IBA1 positivity
396 in the brain (i.e., microgliosis) and microglial activation serving as markers of central nervous
397 system (CNS) inflammation [80-82]. In the hippocampus, $cSiO_2$/VEH/CON mice exhibited
398 pronounced microgliosis, characterized by increased density and altered shape of $IBA1^+$ microglial
399 cells (Figure 11A,B). This neuroinflammatory state was diminished in mice that received CYC,
400 CYC/DHA, and CYC/PDN (Figures 11C, D, and E), and was maximally reduced in mice receiving
401 CYC/DHA+PDN co-therapy, which displayed a more resting microglial appearance (Figure 11F).
402 This was further reflected in markedly lower microgliosis scores for the PDH+DHA co-therapy
403 group, suggesting that the benefits of this combination extends to reduced CNS-related
404 inflammation (Figure 11G).

405

406 **Discussion**

407 LN remains difficult to manage, and there is a significant need for innovative strategies that sustain
408 long-term remission while enabling a meaningful reduction in GC doses. Observational SLE studies
409 have linked higher omega-3 intake and circulating DHA with diminished disease activity as
410 reflected in SLAQ scores and better patient-reported outcomes, including reduced pain and
411 improved sleep [83-85]; however, randomized controlled trials (RCTs) have yielded mixed results.
412 Akbar et al. [22] reported variable benefits across nine RCTs that differed in duration (10–
413 52 weeks), sample size (12–85 participants), and dosage (0.54–3.60 g EPA; 0.30–2.25 g DHA).

414 Several studies reported improvements in clinical or serologic markers [86-90], while others
415 observed only transient or no benefit [32,91-93]. A recent RCT using krill oil (4 g/day; 722 mg EPA,
416 384 mg DHA) showed positive effects in patients with high baseline disease activity (SLEDAI-
417 2K ≥ 9) [16]. Overall, although omega-3 RCTs suggest a potential for modest improvement in SLE
418 disease activity, small sample sizes, inconsistent dosing, varied populations, short follow-up
419 periods, limited assessment of long-term tissue FA incorporation, and suboptimal control of
420 confounding factors hinder clear interpretation. Therefore, the full extent of omega-3s' benefits for
421 individuals with SLE and LN, along with how they interact with standard treatments, remains
422 unclear.

423 Because omega-3 supplements are not patent-protected, large, highly optimized randomized
424 controlled trials used to evaluate new drugs are impractical, stressing the importance of rigorous
425 preclinical models to define their therapeutic potential in LN. In this context, the SALN model offers
426 a stringent, translationally relevant platform for evaluating remission-maintenance strategies after
427 immunosuppressive induction. Mechanistically, short-term, repeated $cSiO_2$ exposure in NZBWF1
428 mice combines an environmentally relevant trigger with genetic susceptibility. Inhaled particles are
429 initially phagocytosed by alveolar macrophages (AMs). This results in phagolysosome
430 destabilization, inflammasome activation, and AM death via pyroptosis and necrosis, and ultimately
431 the release of cytokines, chemokines, DAMPs, nuclear antigens, and $cSiO_2$ into the local
432 environment [78,94] (Figure 12). These events, together with the long pulmonary half-life of $cSiO_2$,
433 create a self-sustaining loop in which dying and activated AMs promote ectopic ELS formation in
434 the lung, enhance T- and B-cell recruitment and activation, and accelerate the production of
435 pathogenic AAbs. This process drives both pulmonary and systemic autoimmunity and results in
436 severe, synchronized glomerulonephritis (GN) that resembles key features of human SLE and LN

437 [55,56]. Compared with the spontaneous NZBWF1 model, SALN presents a condensed,
438 synchronized multi-organ disease course, with LN developing within 3 months after the final $cSiO_2$
439 exposure. This allows intervention studies to be completed in 7 months, rather than 10 to 12 months
440 in the conventional NZBWF1 model.

441 Previous investigations employing SALN have shown that either DHA or PDN monotherapy can
442 prevent LN onset [56-58,60-62,95], but these studies mainly focused on disease prevention. The
443 present study is innovative because it endeavors to bridge this translational gap by using SALN to
444 assess DHA as an adjunct therapy to prolong CYC-induced remission, both alone and in
445 combination with a modest, clinically relevant dose of PDN in established LN. We report for the
446 first time that dietary DHA administered post-LN onset during and after immunosuppressive
447 induction prompts significant remodeling of tissue membrane lipid composition. This change is
448 associated with enhanced clinical and histopathological outcomes (Figure 12). Incorporation of
449 DHA and other omega-3 fatty acids into phospholipids, along with a reciprocal depletion of omega-
450 6 species, most notably ARA, indicates robust reprogramming of tissue lipid pools. In mice given
451 DHA+PDN, increases in total omega-3 and decreases in omega-6 were enhanced by 33 percent and
452 19 percent, respectively, compared with mice fed DHA alone. In the kidney, DHA, particularly
453 when combined with PDN, prolonged CYC-induced remission by delaying proteinuric relapse and
454 maintaining renal structure. This was evidenced by reduced macrophage infiltration, diminished
455 tubular protein deposition, and prevention of ELS formation.

456 The benefits of DHA combined with PDN were observed beyond the kidney. In the lung, this
457 combination reduced perivascular inflammation, ectopic lymphoid aggregates, and local
458 autoantibody production. Systemically, it decreased splenomegaly and circulating autoantibodies.
459 In the brain, DHA+PDN reduced hippocampal microgliosis and improved neural tissue health,

460 indicating a wider impact on neuroinflammatory pathways in the CNS. Collectively, this evidence
461 indicates that DHA-rich nutrition, particularly when combined with PDN, exerts coordinated
462 immune-modulating effects across multiple organs, enhances the durability of LN remission, and
463 reduces extra-renal inflammation and tissue damage, thereby supporting its ability to augment SLE
464 outcomes more broadly. Thus, adjunctive DHA may enhance conventional two-phase
465 immunosuppressive therapy and is consistent with current rheumatology treatment approaches
466 focused on sustained remission with reduced GC exposure [9].

467 The organ-level effects observed here in SALN align with the well-known immunomodulatory
468 actions of omega-3 fatty acids. DHA and other omega-3s affect immune responses through
469 interrelated structural, transcriptional, and metabolic pathways [17,18,96,97]. Their incorporation
470 into membrane phospholipids alters lipid raft organization, increases membrane fluidity, and
471 interferes with receptor clustering required for effective signaling through TLRs, TNFR, and IL1R
472 [98]. At the transcriptional level, DHA suppresses NF-κB and activates PPARγ and NRF2,
473 diminishing oxidative stress and decreasing expression of proinflammatory mediators such as IL6
474 and iNOS [99,100]. Additionally, omega-3s inhibit ARA production from plant-derived LA [101]
475 and competitively inhibit the formation of inflammatory mediators from ARA, such as leukotrienes,
476 prostaglandins, and thromboxanes [96]. DHA also serves as a precursor for proresolving mediators
477 that promote efferocytosis, facilitating the clearance of apoptotic cells and supporting the resolution
478 of chronic inflammation [97]. The evidence presented here is further consistent with preventive
479 studies in NZBWF1 mice exposed to $cSiO_2$, where DHA elicits broad anti-inflammatory and
480 immunoregulatory actions in the lungs [63]. Following a single intranasal $cSiO_2$ challenge, control-
481 fed mice showed increased leukocyte influx, cytokine and chemokine levels, dead cell
482 accumulation, and higher AAbs in BAL. In contrast, DHA-enriched diets lessened these responses,

483 including IL1α, IL6, GM-CSF, CCL2, CCL3, and CXCL10, and lowered autoimmune-related gene
484 signatures linked to type I IFN signaling, TLR activation, and lymphocyte activation, with predicted
485 suppression of regulators like TNFα, IL1β, IFNAR, and IFNγ.

486 The tissue-specific effects of PDN in SALN observed here are in accord with the known
487 immunomodulatory actions of GCs. Treatment with PDN and other synthetic GCs rapidly controls
488 inflammation in SLE and related rheumatic conditions by activating GR, which suppresses NF-
489 κB/AP-1–driven inflammatory pathways in lymphoid and myeloid cells and enhances anti-
490 inflammatory genes like GILZ and DUSP1 [102-104]. Non-genomic GR signaling further
491 contributes by inhibiting PLA2 and activating MAPK and cAMP pathways [102-104]. Additionally,
492 GCs modify lipid rafts by altering their lipid composition and physical properties, disrupting raft
493 formation in some immune cells while also recruiting GRs and related signaling complexes into
494 flotillin- or caveolin-rich raft regions, thereby affecting kinase signaling and gene regulation [105-
495 107]. Thus, the anti-inflammatory effects of DHA and PDN involve multiple parallel interconnected
496 mechanisms.

497 Using SALN, we previously found that pretreatment with a moderate PDN dose (14 mg/day HED),
498 taken orally via diet, significantly reduced $cSiO_2$-induced pulmonary ELS formation, AAb
499 production, and autoimmune gene expression in both the lung and kidney [64]. This treatment also
500 decreased splenomegaly and the severity of glomerulonephritis. Instead of reversing disease
501 signatures, this regimen reduced the magnitude and diversity of transcriptomic changes across
502 organs, showing a general suppression of autoimmune activation. Key adaptive immune modules—
503 including T-cell receptor signaling, antigen presentation, B-cell activation, and Fc-mediated effector
504 pathways—were particularly suppressed, especially in the lung. Overall, these prior findings show
505 that moderate-dose PDN provides widespread but incomplete transcriptional control over the $cSiO_2$-

506 induced autoimmune process, with innate and stress responses still partly active.

507 The PDN dose used in the present study was specifically chosen based on its narrow preventive
508 window in SALN: 14 mg/day HED reduces disease progression, 5 mg/day is ineffective, and
509 46 mg/day causes severe GC-related toxicity without providing a survival benefit [64]. This pattern
510 parallels clinical experience, in which high-dose GCs induce remission but carry significant
511 cumulative toxicity, and highlights that monotherapy suppresses inflammation without restoring
512 immune homeostasis [108]. Based on this prior study, herein we deliberately selected a suboptimal
513 intermediate dose (9.4 mg/day HED), positioned between previously ineffective and minimally
514 effective levels in SALN [64]. Clinically, this dose is near the lower end of moderate-dose GC
515 exposure: in a large SLE cohort, the mean daily PDN-equivalent dose during the first treatment year
516 was 19.4 mg, with about 60% of patients receiving ≥15 mg/day and only 17% maintained below
517 7.5 mg/day [109]. The 9.4 mg/day HED selected here represents a clinically significant exposure,
518 half of the dose usually employed during the first year of treatment, but still above the current treat-
519 to-target guidelines not to exceed 5 to 7.5 mg/day for SLE and LN maintenance.

520 Macrophages play a vital role in SLE development, driven by unresolved tissue inflammation,
521 defective removal of cellular debris, and persistent type I IFN signaling [110-112]. In a recent in
522 vitro study using a novel self-renewing AM model derived from embryonic NZBWF1 mouse liver,
523 we determined that DHA synergistically enhances the suppressive effects of low doses of the water-
524 soluble GC dexamethasone (DEX) on LPS-induced type 1 IFN-driven gene expression [27]. When
525 combined, subinhibitory levels of DHA and DEX led to over tenfold greater gene suppression than
526 either agent alone. This combination significantly reprogrammed inflammatory transcriptional
527 networks, decreasing activity in the NFκB, AP1, IRF, and STAT pathways while promoting
528 pathways associated with resolution and M2 polarization. These in vitro mechanistic insights align

529 with the in vivo SALN results discussed here, further supporting DHA as an adjunct therapy to GC
530 and highlighting its potential to enhance treatment outcomes by targeting critical pathogenic
531 pathways in SLE.

532 Interpretation of these data must consider several limitations. First, the relatively short experimental
533 duration limits conclusions about long-term disease progression and survival, and formal dose–
534 response relationships for both DHA and PDN—individually and together—are yet to be
535 systematically established. Second, the study was intentionally designed to focus on remission
536 maintenance, renal and extrarenal histopathology, and survival rather than a detailed mechanistic
537 analysis of how upstream signaling pathways are affected by DHA and PDN. Third, variations in
538 omega-3 types (DHA vs EPA) and bioavailability (ethyl esters, triglycerides, phospholipids) among
539 formulations on the market may additionally impact treatment effectiveness [16]. Finally, the
540 metabolic and immunological features of SALN may not fully parallel human SLE, so caution is
541 necessary when extrapolating to diverse patient populations. Therefore, to address these limitations,
542 future preclinical research using the SALN model should i) explicitly address dose–response
543 relationships over an extended time period, ii) compare various therapeutic formulations and
544 delivery methods (e.g., structured triglycerides or phospholipid conjugates), and iii) include
545 lipidomic and transcriptomic profiling to understand better how DHA and PDN reprogram immune–
546 metabolic networks across disease. Ultimately, well-designed multicenter clinical trials will be
547 essential to determine the translational relevance and clinical significance of DHA-based adjunctive
548 GC-sparing strategies in SLE and LN.

549 **Conclusion**

550 This study provides compelling preclinical evidence that DHA supplementation significantly
551 enhances the efficacy of PDN in sustaining CYC-induced remission in LN. By leveraging a robust,
552 translationally relevant model, we demonstrate that DHA exerts immunomodulatory effects that
553 complement glucocorticoid mechanisms, resulting in prolonged renal and extrarenal protection.
554 These findings highlight the potential of omega-3 fatty acids as safe, cost-effective adjuncts to
555 conventional immunosuppressive regimens, offering a strategy to reduce glucocorticoid burden
556 while improving long-term outcomes. If validated in clinical trials, DHA-based combination therapy
557 could redefine LN management by integrating precision nutrition into standard care, thereby
558 advancing treatment paradigms toward sustained remission with minimized toxicity.

559

560 Conflict of Interest

561 The authors declare that the research was conducted in the absence of any commercial or financial
562 relationships that could be construed as a potential conflict of interest.

563

564 Author Contributions

565 AA: hypothesis, study design, coordination, animal handling, instillations, urinalysis, necropsy, data
566 curation, data analysis/interpretation, figure preparation, manuscript preparation and submission;
567 OM: animal handling, necropsy, instillations, AAb ELISAs, figure preparation; SJ: animal
568 handling/feeding, injections, urinalysis, diet preparation, sample/data collection, morphometry,
569 figure preparation; JL: animal handling/feeding, diet preparation, data collection; VE: necropsy,
570 BUN assays, figure preparation; JJ: injections, AAb ELISAs; RL: coordinator, instillations,
571 necropsy, sample histology preparation, slide scanning; JW: necropsy, BALF cell counts; JH:

572 necropsy, oversight, lung/kidney/spleen/brain histopathology, semi-quantitative data analysis,
573 manuscript preparation; JP: hypothesis, study design, oversight, funding acquisition, data analysis/
574 interpretation, manuscript preparation, and submission.

575

576

577 **Funding**

578 This research was funded by NIH ES027353 (AA, JP, JH), DOD HT94252510457 (JP, JH), Lupus
579 Research Alliance Grant 1260473 (AA), and Dr. Robert and Carol Deibel Family Endowment (JP).

580

581 **Acknowledgments**

582 The authors thank Amy Porter of the Michigan State University Laboratory for Investigative
583 Histopathology for their assistance with histotechnology.

584

585 **Generative Artificial Intelligence (AI)**

586 Generative AI (Perplexity, Perplexity AI, San Francisco, CA, USA) and Grammarly
587 (Grammarly Inc., San Francisco, CA, USA) were used exclusively for language
588 editing and to improve the clarity, readability, and organization of the manuscript. All
589 scientific content, data interpretation, and conclusions were generated by the authors,
590 who carefully reviewed and edited all AI-assisted text and take full responsibility for
591 the integrity and accuracy of the work

Data Availability Statement

The data supporting the findings of this study are available from the corresponding author upon reasonable request.

597 **Table 1. Formulation of experimental diets.**

Macronutrients[a]	Experimental Diets g/kg Total Diet			
	CON	DHA	PDN	DHA+PDN
Carbohydrates				
Corn Starch	397.486	397.486	397.486	397.486
Maltodextrin (Dyetrose)	132	132	132	132
Sucrose	100	100	100	100
Cellulose	50	50	50	50
Proteins				
Casein	200	200	200	200
L-Cysteine	3	3	3	3
Fats				
Corn Oil[b]	10	10	10	10
High-Oleic Safflower Oil[c]	60	35	60	35
DHA-enriched Algal Oil[d]	0	25	0	25
Essential nutrients				
AIN-93G Mineral Mix	35	35	35	35
AIN-93G Vitamin Mix	10	10	10	10
Choline Bitartrate	2.5	2.5	2.5	2.5
Preservatives				
TBHQ Antioxidant	0.014	0.014	0.014	0.014
Drug				
Prednisone	0	0	0.01	0.01

598 Values in table are shown as mass in g/kg dietAbbreviations: CON: control, DHA: docosahexaenoic acid, PDN:
599 prednisone. . [a]Diet composition is based on the manufacturer's description [65]. [b]Corn oil contributes 6 g/kg diet of
600 linoleic acid and 3 g/kg diet of oleic acid. [c]High-oleic safflower oil contributes 47 g/kg diet of oleic acid and 9 g/kg
601 diet of linoleic acid (https://fdc.nal.usda.gov/). [d]Algal oil contributes 10 g/kg diet of DHA and 4 g/kg diet of oleic
602 acid [113] . A 10 g/kg diet of DHA is calorically equivalent to a human equivalent dose of 5 g/d.

603

604 **Table 2. Relation of mouse CYC injections and dietary PDN to human doses.**
605

Drug	Diet concentration (mg/kg)	Mouse dose (mg/kg bw/d)	HED (mg/kg bw/d)[b]	HED (mg/d)[c]
CYC	0	5	0.4	31.2
PDN	10	1.5[a]	0.12	9.36

606 [a]Mouse dose was calculated by multiplying dietary concentration by the FDA conversion factor of 0.15
607 [114].
608 [b]Human equivalent dose (HED) was calculated by multiplying mouse dose by FDA drug interspecies
609 conversion factor of 0.08 [115].
610 [c]Daily human equivalent dose based on average body weight of 78 kg for women ≥ 20 years of age in
611 the U.S [116]
612

613 **Table 3. Effects of experimental diets on fatty acids in RBCs.**

Chemical Structure	Experimental Group			
	Percent (%) of Total Fatty Acids			
	$cSiO_2$/CYC/CON	$cSiO_2$/CYC/DHA	$cSiO_2$/CYC/PDN	$cSiO_2$/CYC/DHA+PDN
C14:0	0.11 ± 0.02	0.26 ± 0.07**	0.13 ± 0.03	0.30 ± 0.08**
C16:0	25.76 ± 1.6	29.92 ± 0.81****	29.74 ± 1.11	25.76 ± 1.9****
C16:1ω7t	0.05 ± 0.008	0.05 ± 0.005	0.05 ± 0.008	0.05 ± 0.01
C16:1ω7	0.56 ± 0.07	0.67 ± 0.20	0.95 ± 0.22*	1.03 ± 0.20**
C18:0	12.17 ± 1.5	10.83 ± 1.09	10.96 ± 1.53	10.75 ± 0.89
C18:1t	0.12 ± 0.03	0.10 ± 0.02	0.11 ± 0.01	0.08 ± 0.02*
C18:1ω9	23.33 ± 3.56	19.74 ± 1.35	24.63 ± 3.37	17.82 ± 1.26**
C18:2ω6t	0.10 ± 0.02	0.09 ± 0.02	0.14 ± 0.02**	0.09 ± 0.02
C18:2ω6	6.51 ± 1.44	9.14 ± 0.63****	7.49 ± 0.72	8.92 ± 0.89***
C20:0	0.11 ± 0.02	0.10 ± 0.02	0.10 ± 0.01	0.12 ± 0.03
C18:3ω6	0.05 ± 0.02	0.03 ± 0.01*	0.07 ± 0.01**	0.03 ± 0.009*
C20:1ω9	0.46 ± 0.05	0.24 ± 0.02****	0.38 ± 0.08	0.19 ± 0.04****
C18:3ω3	0.01 ± 0	0.01 ± 0.006	0.01 ± 0.007	0.02 ± 0.006
C20:2ω6	0.19 ± 0.04	0.16 ± 0.02	0.16 ± 0.02	0.11 ± 0.02****
C22:0	0.12 ± 0.03	0.14 ± 0.04	0.12 ± 0.02	0.14 ± 0.08
C20:3ω6	1.00 ± 0.10	0.97 ± 0.13	1.14 ± 0.14	0.61 ± 0.13***
C20:4ω6	21.49 ± 2	4.91 ± 0.94****	20.23 ± 2.05	2.40 ± 0.31****
C24:0	0.22 ± 0.06	0.28 ± 0.07	0.23 ± 0.03	0.38 ± 0.06***
C20:5ω3	0.02 ± 0.008	3.66 ± 0.92****	0.03 ± 0.01	5.73 ± 0.85****
C24:1ω9	0.37 ± 0.08	0.35 ± 0.08	0.33 ± 0.04	0.35 ± 0.05
C22:4ω6	2.51 ± 0.57	0.11 ± 0.04**	2.08 ± 0.26	0.04 ± 0.005**
C22:5ω6	2.78 ± 0.70	0.05 ± 0.007**	2.60 ± 0.17	0.03 ± 0.004**
C22:5ω3	0.09 ± 0.03	0.83 ± 0.08****	0.14 ± 0.01	0.91 ± 0.08****
C22:6ω3	1.89 ± 0.23	17.35 ± 1.1****	1.92 ± 0.20	20.17 ± 0.75****
DHA + EPA	1.91 ± 0.24	21.01 ± 1.87****	1.95 ± 0.21	25.9 ± 1.2****
CX:0	38.50 ± 1.65	41.54 ± 0.77**	37.54 ± 1.59	41.42 ± 0.58**
CX:1	24.88 ± 3.51	21.15 ± 1.42	26.46 ± 3.61	19.52 ± 1.4**
CX:≥2ω3	2.01 ± 0.26	21.86 ± 1.93****	2.10 ± 0.21	26.83 ± 1.16****
CX:≥2ω6	34.62 ± 2.51	15.45 ± 1.34****	33.90 ± 2.01	12.24 ± 0.9****

614
615 Fatty acid profiles of RBCs were determined by OmegaQuant Analytics as described in Methods. Data are expressed
616 as mean ± SEM. Symbols: *, **, ***, and **** indicate significant differences at the $p<0.05$, $p<0.01$, $p<0.001$, and
617 $p<0.0001$ levels, respectively.
618

619 # Figure Legends

620 **Figure 1.** Experimental design for determining how diets containing docosahexaenoic acid (DHA) and/or
621 prednisone (PDN) impact the duration of cyclophosphamide (CYC)-induced remission in the silica ($cSiO_2$)-
622 accelerated lupus nephritis (SALN) mouse model. Abbreviations: CON, control diet; VEH, vehicle. Letters: a)
623 nephritis onset/initiate vehicle (VEH) or CYC injections; b) CYC discontinued; c) experiment terminated and mice
624 necropsied when ≥50% CYC-treated CON-fed mice exhibited proteinuria (≥300 mg/dl).

625

626 **Figure 2.** Consumption of DHA and DHA+PDN, but not PDN alone, skews cellular phospholipid profiles in
627 erythrocytes from ω-6 PUFAs to ω-3 PUFAs. Data (mean+/-SEM) are expressed as percent of total fatty acids
628 (TFA). *, **, ***, and **** indicate significant differences at the $p<0.05$, $p<0.01$, $p<0.001$, and $p<0.0001$ levels,
629 respectively.

630

631 **Figure 3.** DHA and PDN monotherapies and co-therapy influence the duration of CYC-induced remission of
632 proteinuria and mortality in the SALN model over the 14-week experimental period. (A) Left panel, percent of
633 mice with significant proteinuria (≥300 mg/dl); right panel, average proteinuria. (B) Average percent of mice with
634 proteinuria (≥300 mg/dl) from weeks 21 to 35. (C) Average proteinuria from weeks 21 to 35. (D) Percent survival
635 as determined using clinical scores indicative of a moribund state as described in Methods. Abbreviations: VEH,
636 vehicle; CON, control diet. Symbols: *, **, ***, and **** indicate significant differences at the $p<0.05$, $p<0.01$,
637 $p<0.001$, and $p<0.0001$ levels, respectively.

638

639 **Figure 4.** DHA and PDN monotherapies and co-therapy prolong CYC-induced diminution of $cSiO_2$-accelerated
640 lupus nephritis. (A-F) Light photomicrographs of Periodic Acid Schiff-stained (PAS) glomeruli (g) and adjacent
641 cortical renal tubules (rt). (B) Membranous glomerular nephritis: dramatic glomerular enlargement with marked
642 thickening of PAS^+ membranous tissue (arrow) and rt with luminal proteinaceous fluid (stippled arrow) in the
643 kidney from the $cSiO_2$/VEH/CON mouse compared to (A) a representative section from a 34-week-old NZBWF1
644 mouse not treated with $cSiO_2$ or drugs obtained from a previous study [61]. These renal lesions are markedly
645 attenuated in the kidney from the (F) $cSiO_2$/CYC/DHA+PDN mouse. Histopathological lesions were scored by

646 pathologist as described in Methods for (G) lupus nephritis, (H) tubular protein, and (I) tubular regeneration.
647 Symbols: #, *, and ** denote statistically significant differences at the $p<0.1$, $p<0.05$, and $p<0.01$ levels,
648 respectively. Solid symbols indicate mice that were taken at the final necropsy at week 35; half-open, half-closed
649 symbols denote moribund mice sacrificed prior to final necropsy.
650
651 **Figure 5.** DHA and PDN co-therapy extends CYC-induced suppression of $cSiO_2$-induced infiltration of
652 inflammatory IBA-1^+ monocyte-derived macrophages in the kidney. (A-F) Representative light photomicrographs
653 of renal cortex immunohistochemically stained for IBA-1^+ monocytes infiltrating peri-tubular and glomerular
654 interstitial tissue (arrows). Panel A is a representative section from a 34-week-old NZBWF1 mouse not treated
655 with $cSiO_2$ or drugs obtained from a previous study [61]. Letters: g, glomeruli; rt, renal tubules. (G) IBA-1^+ areas
656 were quantitatively scored as described in Methods. Symbol: * denotes a statistically significant difference at the
657 $p<0.05$ level. Solid symbols indicate mice that were taken at the final necropsy at week 35; half-open, half-closed
658 symbols denote moribund mice sacrificed prior to final necropsy.
659
660 **Figure 6.** DHA and PDN co-therapy prolongs CYC-induced attenuation of $cSiO_2$-accelerated ectopic lymphoid
661 structure (ELS) development in the kidney. Representative light photomicrographs of (A, B) hematoxylin and
662 eosin (H&E)-stained renal cortex tissue and immunohistochemically stained for (C,D) IBA-1^+, (E,F) $CD3^+$, or
663 (G,H) $CD45R^+$ cells in renal cortex tissue from a (A, C, E, G) nontreated $cSiO_2$/VEH/CON mouse and a (B, D, F,
664 H) co-treated $cSiO_2$/CYC/DHA+PDN mouse. $cSiO_2$-induced renal influx of IBA-1^+ monocytes co-localized with
665 $CD3^+$ and $CD45R^+$ lymphoid cells (T and B cells, respectively) was markedly attenuated in co-treated mouse
666 compared to nontreated mouse. (I) ELS development was semi-quantitatively scored for severity by pathologist
667 as described in Methods. Symbol: * indicates a significant difference at the $p<0.05$ level. . Solid symbols indicate
668 mice that were taken at the final necropsy at week 35; half-open, half-closed symbols denote moribund mice
669 sacrificed prior to final necropsy.
670
671 **Figure 7.** Influence of DHA and PDN monotherapies and co-therapy on $cSiO_2$-induced cellularity and AAbs in
672 bronchoalveolar lavage fluid (BALF). (A) Monocyte, neutrophil, lymphocyte, and total cell accumulation are

673 suppressed by DHA and PDN alone or as co-treatment. Symbols: #, *, **, ***, and **** indicate significant
674 differences at the $p<0.1$, $p<0.05$, $p<0.01$, $p<0.001$, and $p<0.0001$ levels, respectively. (B) IgG AAbs specific for
675 dsDNA and silica-killed cells (SKC) of CYC-treated mice instilled with $cSiO_2$ are modestly suppressed by DHA
676 and PDN co-treatment.
677
678 **Figure 8.** DHA and PDN monotherapies and co-therapy extend CYC-induced attenuation of $cSiO_2$-accelerated
679 ectopic lymphoid structure (ELS) development in the lung. (A-L) Representative light photomicrographs of H&E-
680 stained pulmonary tissue from the left lung lobe. Panels A and B are a representative section from a 34-week-old
681 NZBWF1 mouse not treated with $cSiO_2$ or drugs obtained from a previous study [61]. Peri-vascular ELS (arrows)
682 is markedly attenuated in lung from (K,L) co-therapy $cSiO_2$/CYC/DHA+PDN mouse compared to (C,D)
683 nontreated $cSiO_2$/VEH/CON and (E,F) $cSiO_2$/CYC/CON mice.
684
685 **Figure 9**. DHA and PDN monotherapies and co-therapy prolong CYC-induced reduction of $cSiO_2$-accelerated
686 ectopic lymphoid structure development in the lung. (A, B) ELS development and alveolar proteinosis were semi-
687 quantitatively scored for severity by pathologist as described in Methods. (C, D) $CD3^+$ and $CD45R^+$ cell densities
688 were quantitatively analyzed by digital morphometry as described in Methods. Symbols: *, **, and *** indicate
689 significant differences at the $p<0.05$, $p<0.01$, and $p<0.001$, levels, respectively. . Solid symbols indicate mice that
690 were taken at the final necropsy at week 35; half-open, half-closed symbols denote moribund mice sacrificed prior
691 to final necropsy.
692
693 **Figure 10.** PDN alone or DHA and PDN co-therapy with CYC suppress $cSiO_2$-accelerated splenomegaly. (A-F)
694 Light photomicrographs of H&E-stained splenic tissue. (A) Reference section from a 34-week-old NZBWF1
695 mouse not treated with $cSiO_2$ or drugs obtained from a previous study [61]. (B) Increased white pulp (wp) and
696 reduced red pulp (rp) in splenic tissue from $cSiO_2$/VEH/CON mouse that is markedly attenuated in (F) spleen from
697 mouse receiving $cSiO_2$/CYC/DHA+PDN treatment. Indicators of splenomegaly included (G) spleen weight, (H)
698 white pulp hyperplasia (semi-quantitative scoring by pathologist as described in Methods), and (I) mid cross-
699 sectional area of total spleen (quantitative analysis as described in Methods). (J) Influence of DHA and PDN

700 monotherapies and co-therapy on $cSiO_2$-induced AAbs in plasma. IgG AAbs specific for dsDNA and silica-killed
701 cells (SKC) from CYC-treated mice instilled with $cSiO_2$ are modestly suppressed by PDN treatment alone and by
702 DHA and PDN co-treatment at 33 and 35 weeks. Symbols: #, *, **, and *** indicate significant differences at the
703 $p<0.1$, $p<0.05$, $p<0.01$, and $p<0.001$ levels, respectively. Mice sacrificed prior to final necropsy are indicated by
704 half-open, half-closed symbols, and solid symbols indicate mice that made it to final necropsy at week 35.
705
706 **Figure 11**. DHA and PDN monotherapies and co-therapy prolong CYC suppression of $cSiO_2$-induced
707 microgliosis. Representative photomicrographs of (A) H&E-stained cells and (B-F) immunohistochemically
708 stained for IBA-1^+ microglial cells in the hippocampus of the brain. Microgliosis in the hippocampus from the (B)
709 nontreated $cSiO_2$/VEH/CON mouse is markedly attenuated in (F) co-treated $cSiO_2$/CYC/DHA+PDN mouse. (G)
710 Semi-quantitative severity scoring of microgliosis (IBA-1^+ cells) in the hippocampus as described in Methods.
711 Brains were not taken from moribund mice at necropsy. Symbol: ** indicates a significant difference at the $p<0.01$
712 level.
713
714 **Figure 12.** Schematic summarizing how docosahexaenoic acid (DHA) supplementation influences prednisone
715 (PDN) efficacy for the sustained maintenance of cyclophosphamide-induced remission in silica-triggered lupus.
716 Inhaled crystalline silica ($cSiO_2$) initiates lung cell death and inflammation, inducing damage-associated molecular
717 patterns (DAMPs), autoantigens (AAgs), type I interferons, and chemokines, which together drive robust
718 infiltration by B cells, T cells, and macrophages, leading to ectopic lymphoid structure formation, AAb production,
719 and immune complex (IC) formation. These immunological events in the lung amplify multiorgan pathology,
720 including glomerulonephritis, IBA-1^+ macrophage accumulation, and lymphoid neogenesis in the kidney, splenic
721 lymphoid hyperplasia, and microgliosis in the brain. Compared to single-agent regimens, combined DHA+PDN
722 therapy exerts superior suppression of multisystem lupus pathology (DHA+PDN > PDN = DHA > control for
723 kidney, lung, and brain; DHA+PDN > PDN > DHA > control for spleen), supporting additive benefits of omega-
724 3 supplementation and long-term maintenance with modest steroid doses to reduce risk of flare and cumulative
725 tissue injury. Figure created using BioRender at https://BioRender.com.
726

References

[1] Tsokos GC. The immunology of systemic lupus erythematosus. Nat Immunol. 2024;25(8):1332-1343.

[2] Woo JMP, Parks CG, Jacobsen S, Costenbader KH, Bernatsky S. The role of environmental exposures and gene-environment interactions in the etiology of systemic lupus erythematous. J Intern Med. 2022;291(6):755-778.

[3] Caielli S, Wan Z, Pascual V. Systemic lupus erythematosus pathogenesis: Interferon and beyond. Annu Rev Immunol. 2023;41:533-560.

[4] Hoi A, Igel T, Mok CC, Arnaud L. Systemic lupus erythematosus. Lancet. 2024;403(10441):2326-2338.

[5] Anders HJ, Saxena R, Zhao MH, Parodis I, Salmon JE, et al. Lupus nephritis. Nat Rev Dis Primers. 2020;6(1):7.

[6] Desai NB, Gashti C, Whittier WL. "A change is gonna come" to treatment of lupus nephritis: A review. Am J Kidney Dis. 2025.

[7] Fanouriakis A, Kostopoulou M, Andersen J, Aringer M, Arnaud L, et al. Eular recommendations for the management of systemic lupus erythematosus: 2023 update. Ann Rheum Dis. 2024;83(1):15-29.

[8] Mok CC, Teng YKO, Saxena R, Tanaka Y. Treatment of lupus nephritis: Consensus, evidence and perspectives. Nat Rev Rheumatol. 2023;19(4):227-238.

[9] Frangou E, Anders HJ, Bajema IM, Teng YKO, Malvar A, et al. Immunosuppression withdrawal in patients with lupus nephritis: When, how, and for whom will it be safe? J Am Soc Nephrol. 2024;35(7):955-958.

[10] Newman TV, Guo J, Hernandez I. Emerging treatments for lupus nephritis: Health equity considerations in clinical research and coverage. J Manag Care Spec Pharm. 2021;27(10):1500-1502.

[11] Nicastro HL, Vorkoper S, Sterling R, Korn AR, Brown AGM, et al. Opportunities to advance implementation science and nutrition research: A commentary on the strategic plan for nih nutrition research. Transl Behav Med. 2023;13(1):1-6.

[12] Shanmugam VK, Ufret-Vincenty C, Li X, Clayton JA. The inaugural nih-wide strategic plan for autoimmune disease research (fy2026–2030). Arthr Rheumatol.n/a(n/a):4.

[13] Robinson GA, McDonnell T, Wincup C, Martin-Gutierrez L, Wilton J, et al. Diet and lupus: What do the patients think? Lupus. 2019;28(6):755-763.

[14] Ramessar N, Borad A, Schlesinger N. The effect of omega-3 fatty acid supplementation in systemic lupus erythematosus patients: A systematic review. Lupus. 2022;31(3):287-296.

[15] Salek M, Hosseini Hooshiar S, Salek M, Poorebrahimi M, Jafarnejad S. Omega-3 fatty acids: Current insights into mechanisms of action in systemic lupus erythematosus. Lupus. 2023;32(1):7-22.

[16] Salmon J, Wallace DJ, Rus V, Cox A, Dykas C, et al. Correction of omega-3 fatty acid deficiency and improvement in disease activity in patients with systemic lupus erythematosus treated with krill oil concentrate: A multicentre, randomised, double-blind, placebo-controlled trial. Lupus Sci Med. 2024;11(2).

[17] Calder PC. Omega-3 fatty acids and inflammatory processes: From molecules to man. Biochem Soc Trans. 2017;45(5):1105-1115.

[18] Bodur M, Yilmaz B, Ağagündüz D, Ozogul Y. Immunomodulatory effects of omega-3 fatty acids: Mechanistic insights and health implications. Mol Nutr Food Res. 2025;69(10):e202400752.
[19] Djuricic I, Calder PC. Pros and cons of long-chain omega-3 polyunsaturated fatty acids in cardiovascular health. Annu Rev Pharmacol Toxicol. 2023;63:383-406.
[20] Laguzzi F, Åkesson A, Marklund M, Qian F, Gigante B, et al. Role of polyunsaturated fat in modifying cardiovascular risk associated with family history of cardiovascular disease: Pooled de novo results from 15 observational studies. Circulation. 2024;149(4):305-316.
[21] O'Keefe JH, Tintle NL, Harris WS, O'Keefe EL, Sala-Vila A, et al. Omega-3 blood levels and stroke risk: A pooled and harmonized analysis of 183 291 participants from 29 prospective studies. Stroke. 2024;55(1):50-58.
[22] Akbar U, Yang M, Kurian D, Mohan C. Omega-3 fatty acids in rheumatic diseases: A critical review. J Clin Rheumatol. 2017;23(6):330-339.
[23] Sigaux J, Mathieu S, Nguyen Y, Sanchez P, Letarouilly JG, et al. Impact of type and dose of oral polyunsaturated fatty acid supplementation on disease activity in inflammatory rheumatic diseases: A systematic literature review and meta-analysis. Arthritis Res Ther. 2022;24(1):100.
[24] EFSA Panel on Dietetic Products N, Allergies. Scientific opinion on the tolerable upper intake level of eicosapentaenoic acid (epa), docosahexaenoic acid (dha) and docosapentaenoic acid (dpa). EFSA Journal. 2012;10(7):2815.
[25] Kennedy ET, Luo H, Ausman LM. Cost implications of alternative sources of (n-3) fatty acid consumption in the united states1234. The Journal of Nutrition. 2012;142(3):605S-609S.
[26] Wierenga KA, Strakovsky RS, Benninghoff AD, Rajasinghe LD, Lock AL, et al. Requisite omega-3 hufa biomarker thresholds for preventing murine lupus flaring. Front Immunol. 2020;11:1796.
[27] Heine LK, Nault R, Jackson J, Anderson AN, Harkema JR, et al. Omega-3 fatty acid synergy with glucocorticoid in mouse lupus macrophage model: Targeting pathogenic pathways to reduce steroid dependence. Frontiers in Immunology. 2025;Volume 16 - 2025.
[28] Alexander NJ, Smythe NL, Jokinen MP. The type of dietary fat affects the severity of autoimmune disease in nzb/nzw mice. Am J Pathol. 1987;127(1):106-21.
[29] Bhattacharya A, Lawrence RA, Krishnan A, Zaman K, Sun D, et al. Effect of dietary n-3 and n-6 oils with and without food restriction on activity of antioxidant enzymes and lipid peroxidation in livers of cyclophosphamide treated autoimmune-prone nzb/w female mice. J Am Coll Nutr. 2003;22(5):388-99.
[30] Blok WL, Katan MB, van der Meer JW. Modulation of inflammation and cytokine production by dietary (n-3) fatty acids. J Nutr. 1996;126(6):1515-33.
[31] Chandrasekar B, Troyer DA, Venkatraman JT, Fernandes G. Dietary omega-3 lipids delay the onset and progression of autoimmune lupus nephritis by inhibiting transforming growth factor beta mrna and protein expression. J Autoimmun. 1995;8(3):381-93.
[32] Clark WF, Parbtani A. Omega-3 fatty acid supplementation in clinical and experimental lupus nephritis. Am J Kidney Dis. 1994;23(5):644-7.
[33] Fernandes G, Bysani C, Venkatraman JT, Tomar V, Zhao W. Increased tgf-beta and decreased oncogene expression by omega-3 fatty acids in the spleen delays onset of autoimmune disease in b/w mice. J Immunol. 1994;152(12):5979-87.
[34] Fernandes G, Chandrasekar B, Luan X, Troyer DA. Modulation of antioxidant enzymes and programmed cell death by n-3 fatty acids. Lipids. 1996;31 Suppl(3 SUPPL.):S91-6.

[35] Godfrey DG, Stimson WH, Watson J, Belch JF, Sturrock RD. Effects of dietary supplementation on autoimmunity in the mrl/lpr mouse: A preliminary investigation. Ann Rheum Dis. 1986;45(12):1019-24.
[36] Halade GV, Rahman MM, Bhattacharya A, Barnes JL, Chandrasekar B, et al. Docosahexaenoic acid-enriched fish oil attenuates kidney disease and prolongs median and maximal life span of autoimmune lupus-prone mice. J Immunol. 2010;184(9):5280-6.
[37] Halade GV, Williams PJ, Veigas JM, Barnes JL, Fernandes G. Concentrated fish oil (lovaza(r)) extends lifespan and attenuates kidney disease in lupus-prone short-lived (nzbxnzw)f1 mice. Exp Biol Med (Maywood). 2013;238(6):610-22.
[38] Jolly CA, Fernandes G. Diet modulates th-1 and th-2 cytokine production in the peripheral blood of lupus-prone mice. J Clin Immunol. 1999;19(3):172-8.
[39] Jolly CA, Muthukumar A, Reddy Avula CP, Fernandes G. Maintenance of nf-kappab activation in t-lymphocytes and a naive t-cell population in autoimmune-prone (nzb/nzw)f(1) mice by feeding a food-restricted diet enriched with n-3 fatty acids. Cell Immunol. 2001;213(2):122-33.
[40] Kelley VE, Ferretti A, Izui S, Strom TB. A fish oil diet rich in eicosapentaenoic acid reduces cyclooxygenase metabolites, and suppresses lupus in mrl-lpr mice. J Immunol. 1985;134(3):1914-9.
[41] Kobayashi A, Ito A, Shirakawa I, Tamura A, Tomono S, et al. Dietary supplementation with eicosapentaenoic acid inhibits plasma cell differentiation and attenuates lupus autoimmunity. Front Immunol. 2021;12:650856.
[42] Lim BO, Jolly CA, Zaman K, Fernandes G. Dietary (n-6) and (n-3) fatty acids and energy restriction modulate mesenteric lymph node lymphocyte function in autoimmune-prone (nzb x nzw)f1 mice. J Nutr. 2000;130(7):1657-64.
[43] Cheng Y, Liu L, Ye Y, He Y, Hu W, et al. Roles of macrophages in lupus nephritis. Front Pharmacol. 2024;15:1477708.
[44] Pestka JJ, Vines LL, Bates MA, He K, Langohr I. Comparative effects of n-3, n-6 and n-9 unsaturated fatty acid-rich diet consumption on lupus nephritis, autoantibody production and cd4+ t cell-related gene responses in the autoimmune nzbwf1 mouse. PLoS One. 2014;9(6):e100255.
[45] Prickett JD, Robinson DR, Steinberg AD. A diet enriched with eicosapentaenoic acid suppresses autoimmune nephritis in female (nzb x nzw) f1 mice. Trans Assoc Am Physicians. 1982;95:145-54.
[46] Reddy Avula CP, Lawrence RA, Zaman K, Fernandes G. Inhibition of intracellular peroxides and apoptosis of lymphocytes in lupus-prone b/w mice by dietary n-6 and n-3 lipids with calorie restriction. J Clin Immunol. 2002;22(4):206-19.
[47] Robinson DR, Hirai A, Steinberg AD, Colvin RB. Alleviation of murine autoimmune disease by dietary marine lipids. Adv Prostaglandin Thromboxane Leukot Res. 1987;17B:850-3.
[48] Robinson DR, Prickett JD, Polisson R, Steinberg AD, Levine L. The protective effect of dietary fish oil on murine lupus. Prostaglandins. 1985;30(1):51-75.
[49] Robinson DR, Xu LL, Tateno S, Guo M, Colvin RB. Suppression of autoimmune disease by dietary n-3 fatty acids. J Lipid Res. 1993;34(8):1435-44.
[50] Spurney RF, Ruiz P, Albrightson CR, Pisetsky DS, Coffman TM. Fish oil feeding modulates leukotriene production in murine lupus nephritis. Prostaglandins. 1994;48(5):331-48.

[51] Venkatraman JT, Chu WC. Effects of dietary omega-3 and omega-6 lipids and vitamin e on serum cytokines, lipid mediators and anti-DNA antibodies in a mouse model for rheumatoid arthritis. J Am Coll Nutr. 1999;18(6):602-13.
[52] Watson J, Godfrey D, Stimson WH, Belch JJ, Sturrock RD. The therapeutic effects of dietary fatty acid supplementation in the autoimmune disease of the mrl-mp-lpr/lpr mouse. Int J Immunopharmacol. 1988;10(4):467-71.
[53] Westberg G, Tarkowski A, Svalander C. Effect of eicosapentaenoic acid rich menhaden oil and maxepa on the autoimmune disease of mrl/l mice. Int Arch Allergy Appl Immunol. 1989;88(4):454-61.
[54] Bates MA, Brandenberger C, Langohr I, Kumagai K, Harkema JR, et al. Silica triggers inflammation and ectopic lymphoid neogenesis in the lungs in parallel with accelerated onset of systemic autoimmunity and glomerulonephritis in the lupus-prone nzbwf1 mouse. PLoS One. 2015;10(5):e0125481.
[55] Bates MA, Benninghoff AD, Gilley KN, Holian A, Harkema JR, et al. Mapping of dynamic transcriptome changes associated with silica-triggered autoimmune pathogenesis in the lupus-prone nzbwf1 mouse. Front Immunol. 2019;10:632.
[56] Bates MA, Brandenberger C, Langohr, II, Kumagai K, Lock AL, et al. Silica-triggered autoimmunity in lupus-prone mice blocked by docosahexaenoic acid consumption. PLoS One. 2016;11(8):e0160622.
[57] Bates MA, Akabari P, Gilley KN, Wagner JG, Li N, et al. Dietary docosahexaenoic acid prevents silica-induced development of pulmonary ectopic germinal centers and glomerulonephritis in the lupus-prone nzbwf1 mouse. Front Immunol. 2018;9:2002.
[58] Benninghoff AD, Bates MA, Chauhan PS, Wierenga KA, Gilley KN, et al. Docosahexaenoic acid consumption impedes early interferon- and chemokine-related gene expression while suppressing silica-triggered flaring of murine lupus. Front Immunol. 2019;10:2851.
[59] Gilley KN, Wierenga KA, Chauhuan PS, Wagner JG, Lewandowski RP, et al. Influence of total western diet on docosahexaenoic acid suppression of silica-triggered lupus flaring in nzbwf1 mice. PLoS One. 2020;15(5):e0233183.
[60] Rajasinghe LD, Li QZ, Zhu C, Yan M, Chauhan PS, et al. Omega-3 fatty acid intake suppresses induction of diverse autoantibody repertoire by crystalline silica in lupus-prone mice. Autoimmunity. 2020;53(7):415-433.
[61] Pestka JJ, Akbari P, Wierenga KA, Bates MA, Gilley KN, et al. Omega-3 polyunsaturated fatty acid intervention against established autoimmunity in a murine model of toxicant-triggered lupus. Front Immunol. 2021;12:653464.
[62] Rajasinghe LD, Bates MA, Benninghoff AD, Wierenga KA, Harkema JR, et al. Silica induction of diverse inflammatory proteome in lungs of lupus-prone mice quelled by dietary docosahexaenoic acid supplementation. Front Immunol. 2021;12:781446.
[63] Chauhan PS, Benninghoff AD, Favor OK, Wagner JG, Lewandowski RP, et al. Dietary docosahexaenoic acid supplementation inhibits acute pulmonary transcriptional and autoantibody responses to a single crystalline silica exposure in lupus-prone mice. Front Immunol. 2024;15:1275265.
[64] Heine LK, Benninghoff AD, Ross EA, Rajasinghe LD, Wagner JG, et al. Comparative effects of human-equivalent low, moderate, and high dose oral prednisone intake on autoimmunity and glucocorticoid-related toxicity in a murine model of environmental-triggered lupus. Front Immunol. 2022;13:972108.

[65] Reeves PG, Nielsen FH, Fahey GC, Jr. Ain-93 purified diets for laboratory rodents: Final report of the american institute of nutrition ad hoc writing committee on the reformulation of the ain-76a rodent diet. J Nutr. 1993;123(11):1939-51.

[66] Buttgereit F, Da Silva JAP, Boers M, Burmester GR, Cutolo M, et al. Standardised nomenclature for glucocorticoid dosages and glucocorticoid treatment regimens: Current questions and tentative answers in rheumatology. Annals of the Rheumatic Diseases. 2002;61(8):718-722.

[67] Osha's final rule to protect workers from exposure to respirable crystalline silica, (2016).

[68] Bankhead P, Loughrey MB, Fernández JA, Dombrowski Y, McArt DG, et al. Qupath: Open source software for digital pathology image analysis. Sci Rep. 2017;7(1):16878.

[69] Meyerholz DK, Beck AP. Fundamental concepts for semiquantitative tissue scoring in translational research. Ilar j. 2018;59(1):13-17.

[70] McDonald OF, Wagner JG, Lewandowski RP, Heine LK, Estrada V, et al. Impact of soluble epoxide hydrolase inhibition on silica-induced pulmonary fibrosis, ectopic lymphoid neogenesis, and autoantibody production in lupus-prone mice. Inhal Toxicol. 2024;36(7-8):442-460.

[71] Harris WS. Recent studies confirm the utility of the omega-3 index. Curr Opin Clin Nutr Metab Care. 2025;28(2):91-95.

[72] Ohsawa K, Imai Y, Sasaki Y, Kohsaka S. Microglia/macrophage-specific protein iba1 binds to fimbrin and enhances its actin-bundling activity. J Neurochem. 2004;88(4):844-56.

[73] Wang M, Rajkumar S, Lai Y, Liu X, He J, et al. Tertiary lymphoid structures as local perpetuators of organ-specific immune injury: Implication for lupus nephritis. Front Immunol. 2023;14:1204777.

[74] Masum MA, Ichii O, Elewa YHA, Otani Y, Namba T, et al. Vasculature-associated lymphoid tissue: A unique tertiary lymphoid tissue correlates with renal lesions in lupus nephritis mouse model. Front Immunol. 2020;11:595672.

[75] Dorraji SE, Kanapathippillai P, Hovd AK, Stenersrød MR, Horvei KD, et al. Kidney tertiary lymphoid structures in lupus nephritis develop into large interconnected networks and resemble lymph nodes in gene signature. Am J Pathol. 2020;190(11):2203-2225.

[76] Harbeck RJ, Launder T, Staszak C. Mononuclear cell pulmonary vasculitis in nzb/w mice. Ii. Immunohistochemical characterization of the infiltrating cells. Am J Pathol. 1986;123(2):204-11.

[77] Staszak C, Harbeck RJ. Mononuclear-cell pulmonary vasculitis in nzb/w mice. I. Histopathologic evaluation of spontaneously occurring pulmonary infiltrates. Am J Pathol. 1985;120(1):99-105.

[78] Wierenga KA, Harkema JR, Pestka JJ. Lupus, silica, and dietary omega-3 fatty acid interventions. Toxicol Pathol. 2019;47(8):1004-1011.

[79] Ye YL, Chiang BL. Reconstitution of severe combined immunodeficient mice with spleen cells from autoimmune nzbxnzw f1 mice. Clin Exp Rheumatol. 1998;16(1):33-7.

[80] Nikolopoulos D, Manolakou T, Polissidis A, Filia A, Bertsias G, et al. Microglia activation in the presence of intact blood-brain barrier and disruption of hippocampal neurogenesis via il-6 and il-18 mediate early diffuse neuropsychiatric lupus. Ann Rheum Dis. 2023;82(5):646-657.

[81] Nomura A, Noto D, Murayama G, Chiba A, Miyake S. Unique primed status of microglia under the systemic autoimmune condition of lupus-prone mice. Arthritis Res Ther. 2019;21(1):303.

[82] Rodríguez-Gómez JA, Kavanagh E, Engskog-Vlachos P, Engskog MKR, Herrera AJ, et al. Microglia: Agents of the cns pro-inflammatory response. Cells. 2020;9(7):1717.
[83] Charoenwoodhipong P, Harlow SD, Marder W, Hassett AL, McCune WJ, et al. Dietary omega polyunsaturated fatty acid intake and patient-reported outcomes in systemic lupus erythematosus: The michigan lupus epidemiology and surveillance program. Arthritis Care Res (Hoboken). 2020;72(7):874-881.
[84] Vordenbaumen S, Sokolowski A, Kutzner L, Rund KM, Dusing C, et al. Erythrocyte membrane polyunsaturated fatty acid profiles are associated with systemic inflammation and fish consumption in systemic lupus erythematosus: A cross-sectional study. Lupus. 2020;29(6):554-559.
[85] Gilley KF, JI; Zick, SM; Li, K; , Wang LM, W; , Mccune WJ, R; Herndon-Fenton,S; Hassett,A; Barbour, K; Pestka, J.J.;Somers, EC;. Serum fatty acid profiles in systemic lupus erythematosus and patient reported outcomes: The michigan lupus epidemiology & surveillance (miles) program. Frontiers in Immunology. 2024;15.
[86] Arriens C, Hynan LS, Lerman RH, Karp DR, Mohan C. Placebo-controlled randomized clinical trial of fish oil's impact on fatigue, quality of life, and disease activity in systemic lupus erythematosus. Nutr J. 2015;14:82.
[87] Duffy EM, Meenagh GK, McMillan SA, Strain JJ, Hannigan BM, et al. The clinical effect of dietary supplementation with omega-3 fish oils and/or copper in systemic lupus erythematosus. J Rheumatol. 2004;31(8):1551-6.
[88] Lozovoy MA, Simão AN, Morimoto HK, Scavuzzi BM, Iriyoda TV, et al. Fish oil n-3 fatty acids increase adiponectin and decrease leptin levels in patients with systemic lupus erythematosus. Mar Drugs. 2015;13(2):1071-83.
[89] Walton AJ, Snaith ML, Locniskar M, Cumberland AG, Morrow WJ, et al. Dietary fish oil and the severity of symptoms in patients with systemic lupus erythematosus. Ann Rheum Dis. 1991;50(7):463-6.
[90] Wright SA, O'Prey FM, McHenry MT, Leahey WJ, Devine AB, et al. A randomised interventional trial of omega-3-polyunsaturated fatty acids on endothelial function and disease activity in systemic lupus erythematosus. Ann Rheum Dis. 2008;67(6):841-8.
[91] Westberg G, Tarkowski A. Effect of maxepa in patients with sle. A double-blind, crossover study. Scand J Rheumatol. 1990;19(2):137-43.
[92] Bello KJ, Fang H, Fazeli P, Bolad W, Corretti M, et al. Omega-3 in sle: A double-blind, placebo-controlled randomized clinical trial of endothelial dysfunction and disease activity in systemic lupus erythematosus. Rheumatol Int. 2013;33(11):2789-96.
[93] Clark WF, Parbtani A, Huff MW, Reid B, Holub BJ, et al. Omega-3 fatty acid dietary supplementation in systemic lupus erythematosus. Kidney Int. 1989;36(4):653-60.
[94] Favor OK, Pestka JJ, Bates MA, Lee KSS. Centrality of myeloid-lineage phagocytes in particle-triggered inflammation and autoimmunity. Frontiers in Toxicology. 2021;Volume 3 - 2021.
[95] Heine LK, Scarlett T, Wagner JG, Lewandowski RP, Benninghoff AD, et al. Crystalline silica-induced pulmonary inflammation and autoimmunity in mature adult nzbw/f1 mice: Age-related sensitivity and impact of omega-3 fatty acid intervention. Inhal Toxicol. 2024;36(2):106-123.
[96] Calder PC. Omega-3 polyunsaturated fatty acids and inflammatory processes: Nutrition or pharmacology? Br J Clin Pharmacol. 2013;75(3):645-62.
[97] Djuricic I, Calder PC. Beneficial outcomes of omega-6 and omega-3 polyunsaturated fatty acids on human health: An update for 2021. Nutrients. 2021;13(7):2421.

[98] Pennington ER, Virk R, Bridges MD, Bathon BE, Beatty N, et al. Docosahexaenoic acid controls pulmonary macrophage lipid raft size and inflammation. J Nutr. 2024;154(6):1945-1958.
[99] Wierenga KA, Riemers FM, Westendorp B, Harkema JR, Pestka JJ. Single cell analysis of docosahexaenoic acid suppression of sequential lps-induced proinflammatory and interferon-regulated gene expression in the macrophage. Front Immunol. 2022;13:993614.
[100] Chang HY, Lee HN, Kim W, Surh YJ. Docosahexaenoic acid induces m2 macrophage polarization through peroxisome proliferator-activated receptor gamma activation. Life Sci. 2015;120:39-47.
[101] Ralston JC, Matravadia S, Gaudio N, Holloway GP, Mutch DM. Polyunsaturated fatty acid regulation of adipocyte fads1 and fads2 expression and function. Obesity. 2015;23(4):725-728.
[102] Furst R, Schroeder T, Eilken HM, Bubik MF, Kiemer AK, et al. Mapk phosphatase-1 represents a novel anti-inflammatory target of glucocorticoids in the human endothelium. FASEB J. 2007;21(1):74-80.
[103] Cain DW, Cidlowski JA. Immune regulation by glucocorticoids. Nature Publishing Group; 2017. p. 233-247.
[104] Vandewalle J, Luypaert A, De Bosscher K, Libert C. Therapeutic mechanisms of glucocorticoids. Trends Endocrinol Metab. 2018;29(1):42-54.
[105] Atkovska K, Klingler J, Oberwinkler J, Keller S, Hub JS. Rationalizing steroid interactions with lipid membranes: Conformations, partitioning, and kinetics. ACS Cent Sci. 2018;4(9):1155-1165.
[106] Yamagata S, Tomita K, Sano H, Itoh Y, Fukai Y, et al. Non-genomic inhibitory effect of glucocorticoids on activated peripheral blood basophils through suppression of lipid raft formation. Clin Exp Immunol. 2012;170(1):86-93.
[107] Van Laethem F, Liang X, Andris F, Urbain J, Vandenbranden M, et al. Glucocorticoids alter the lipid and protein composition of membrane rafts of a murine t cell hybridoma. J Immunol. 2003;170(6):2932-9.
[108] Mok TC, Mok CC. Glucocorticoid in systemic lupus erythematosus: The art beyond science. Expert Rev Clin Immunol. 2025;21(5):543-553.
[109] Birt JA, Wu J, Griffing K, Bello N, Princic N, et al. Corticosteroid dosing and opioid use are high in patients with sle and remain elevated after belimumab initiation: A retrospective claims database analysis. Lupus Sci Med. 2020;7(1).
[110] Li Y, Lee PY, Reeves WH. Monocyte and macrophage abnormalities in systemic lupus erythematosus. Arch Immunol Ther Exp (Warsz). 2010;58(5):355-64.
[111] Udalova IA, Mantovani A, Feldmann M. Macrophage heterogeneity in the context of rheumatoid arthritis. Nat Rev Rheumatol. 2016;12(8):472-85.
[112] Northcott M, Jones S, Koelmeyer R, Bonin J, Vincent F, et al. Type 1 interferon status in systemic lupus erythematosus: A longitudinal analysis. Lupus Sci Med. 2022;9(1):e000625.
[113] USFDA. Gras notice (grn) no. 553: Algal oil (40% docosahexaenoic acid) derived from schizochytrium sp. Silver Spring, MD: U.S. Food and Drug Administration, Center for Food Safety and Applied Nutrition; 2015.
[114] Lehman AJ. Approximate relation of parts per million in the diet to mg/kg bw/day. Association of Food and Drug Officials Quarterly Bulletin. 1954 18.
[115] FDA. Estimating the safe starting dose in clinical trials for therapeutics in adult healthy volunteers.: U.S. Department of Health and Human Services 2005. Available from: https://www.fda.gov/regulatory-information/search-fda-guidance-documents/estimating-maximum-safe-starting-dose-initial-clinical-trials-therapeutics-adult-healthy-volunteers

[116] Fryar C, Carroll M, Gu Q, Afful J, Ogden C. Anthropometric reference data for children and adults: United states, 2015–2018. National Center for Health Statistics Vital Health Stat 2021;3(46).

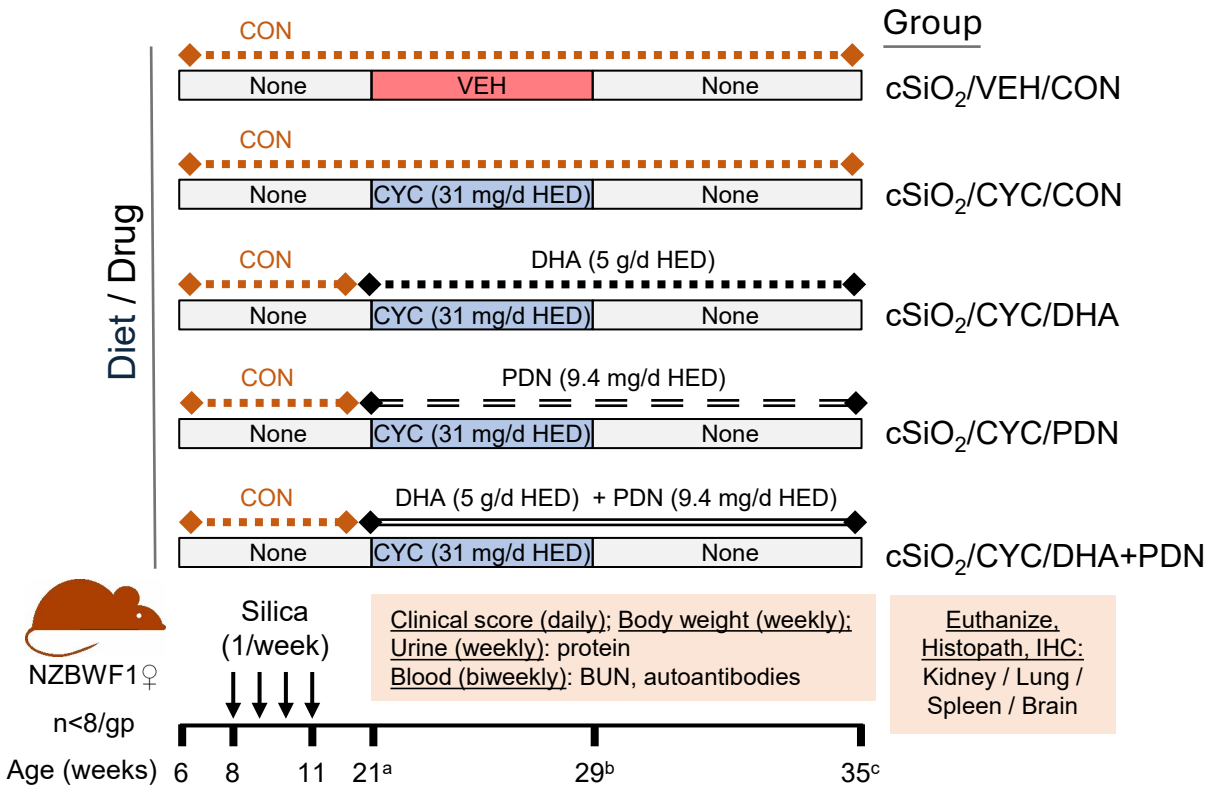
Group
Diet / Drug
CON
None
VEH
None
cSiO2/VEH/CON
CON
None
CYC (31 mg/d HED)
None
cSiO2/CYC/CON
CON
DHA (5 g/d HED)
None
CYC (31 mg/d HED)
None
cSiO2/CYC/DHA
CON
PDN (9.4 mg/d HED)
None
CYC (31 mg/d HED)
None
cSiO2/CYC/PDN
CON
DHA (5 g/d HED) + PDN (9.4 mg/d HED)
None
CYC (31 mg/d HED)
None
cSiO2/CYC/DHA+PDN
NZBWF1♀
n<8/gp
Silica
(1/week)
Clinical score (daily); Body weight (weekly);
Urine (weekly): protein
Blood (biweekly): BUN, autoantibodies
Euthanize,
Histopath, IHC:
Kidney / Lung /
Spleen / Brain
Age (weeks) 6 8 11 21a 29b 35c

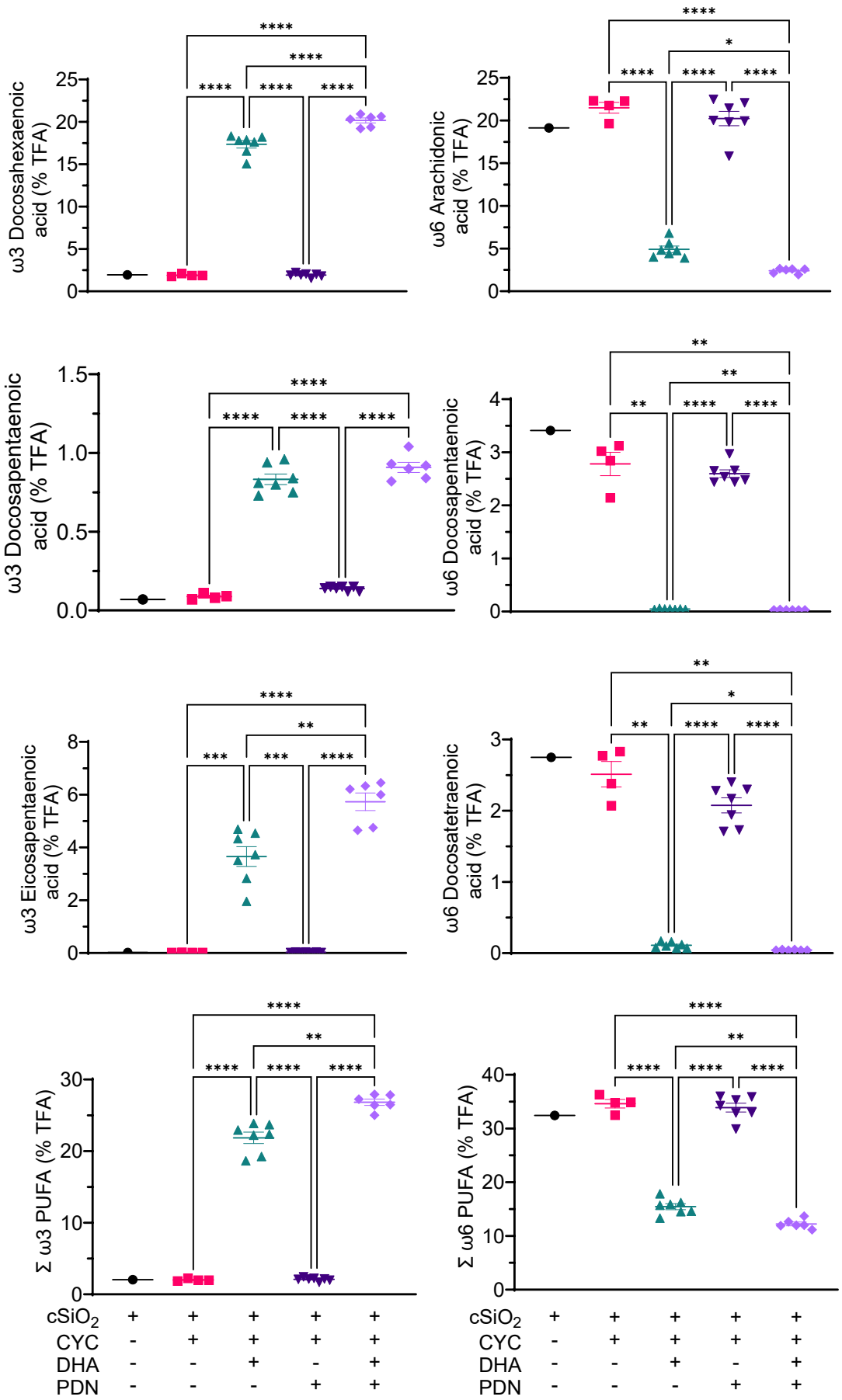
ω3 Docosahexaenoic acid (% TFA)
ω6 Arachidonic acid (% TFA)
ω3 Docosapentaenoic acid (% TFA)
ω6 Docosapentaenoic acid (% TFA)
ω3 Eicosapentaenoic acid (% TFA)
ω6 Docosatetraenoic acid (% TFA)
Σ ω3 PUFA (% TFA)
Σ ω6 PUFA (% TFA)
cSiO2 + + + + +
CYC - + + + +
DHA - - + - +
PDN - - - + +

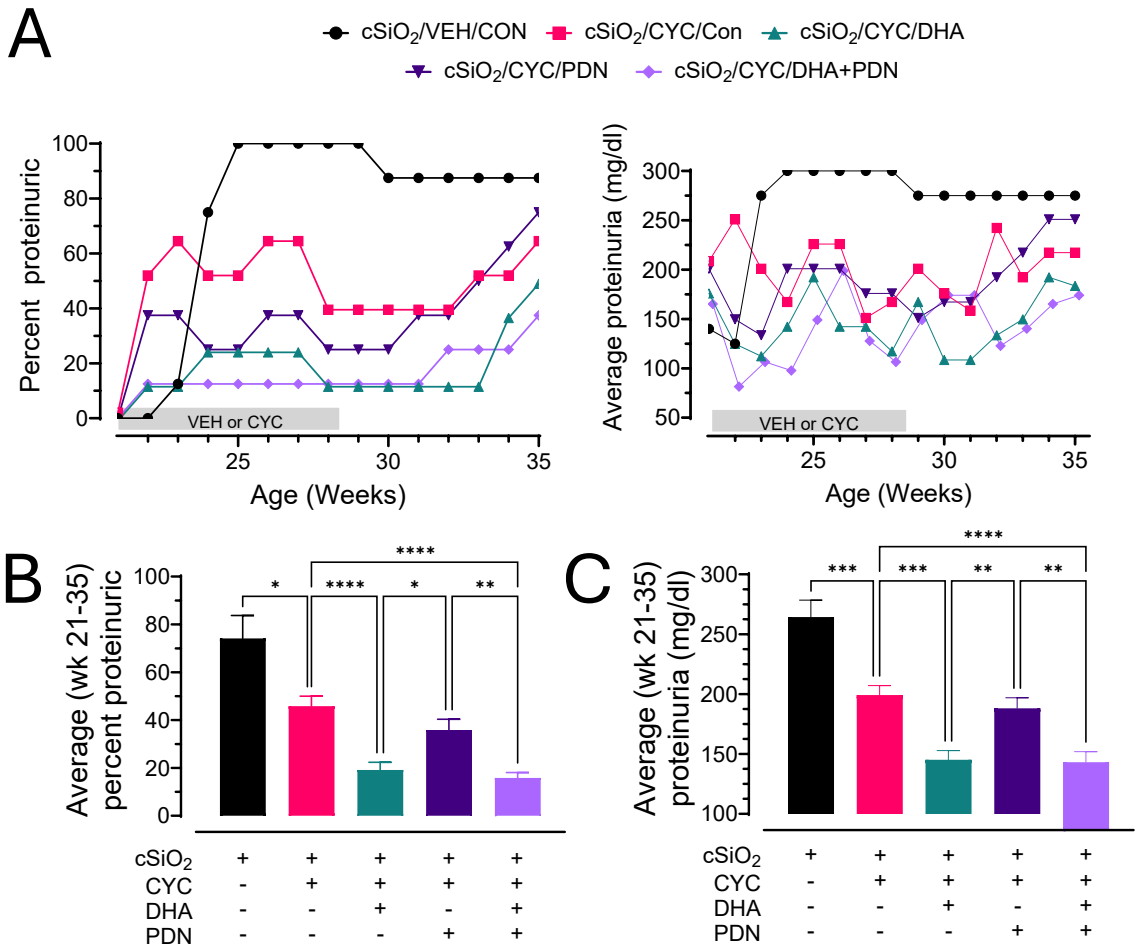
A
cSiO2/VEH/CON
cSiO2/CYC/Con
cSiO2/CYC/DHA
cSiO2/CYC/PDN
cSiO2/CYC/DHA+PDN
Percent proteinuric
Average proteinuria (mg/dl)
VEH or CYC
Age (Weeks)
B
Average (wk 21-35) percent proteinuric
C
Average (wk 21-35) proteinuria (mg/dl)
cSiO2
CYC
DHA
PDN

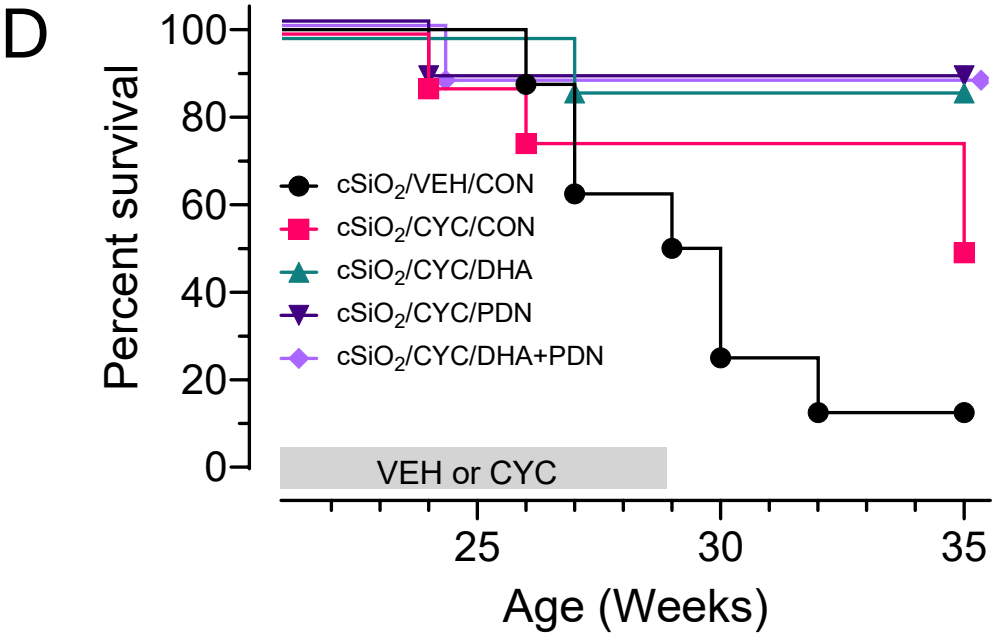
D
Percent survival
cSiO2/VEH/CON
cSiO2/CYC/CON
cSiO2/CYC/DHA
cSiO2/CYC/PDN
cSiO2/CYC/DHA+PDN
VEH or CYC
Age (Weeks)

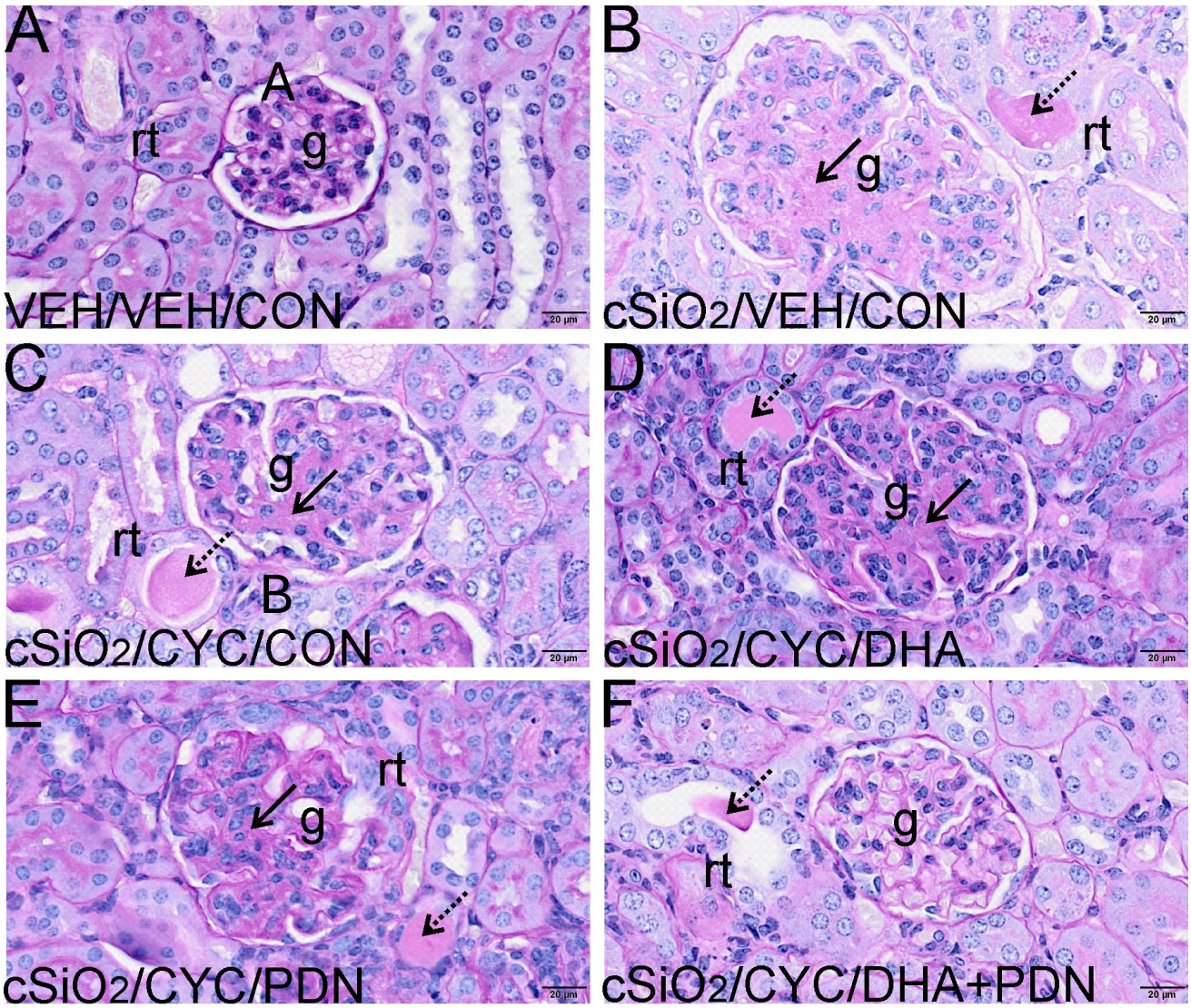
A
A
rt
g
VEH/VEH/CON
20 µm
B
rt
g
cSiO2/VEH/CON
20 µm
C
g
rt
B
cSiO2/CYC/CON
20 µm
D
rt
g
cSiO2/CYC/DHA
20 µm
E
rt
g
cSiO2/CYC/PDN
20 µm
F
g
rt
cSiO2/CYC/DHA+PDN
20 µm

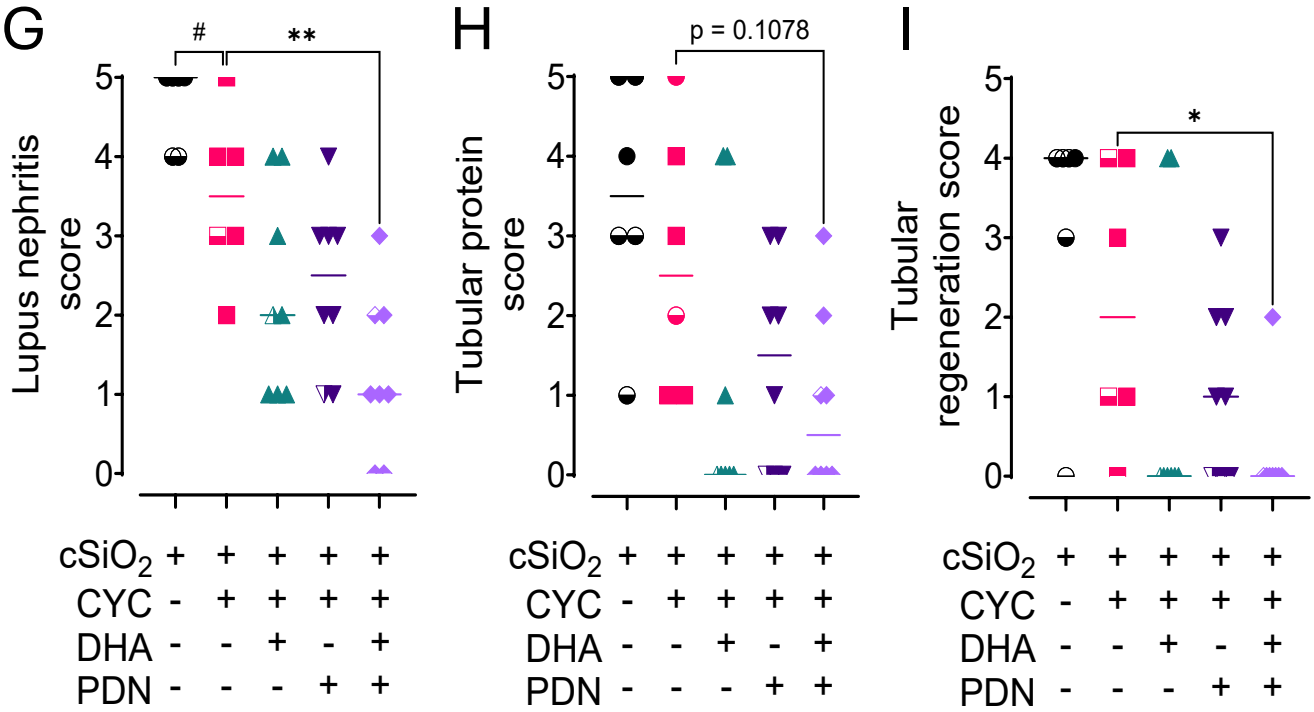
G
#
**
Lupus nephritis score
0
1
2
3
4
5
cSiO2 + + + + +
CYC - + + + +
DHA - - + - +
PDN - - - + +
H
p = 0.1078
Tubular protein score
0
1
2
3
4
5
cSiO2 + + + + +
CYC - + + + +
DHA - - + - +
PDN - - - + +
I
*
Tubular regeneration score
0
1
2
3
4
5
cSiO2 + + + + +
CYC - + + + +
DHA - - + - +
PDN - - - + +

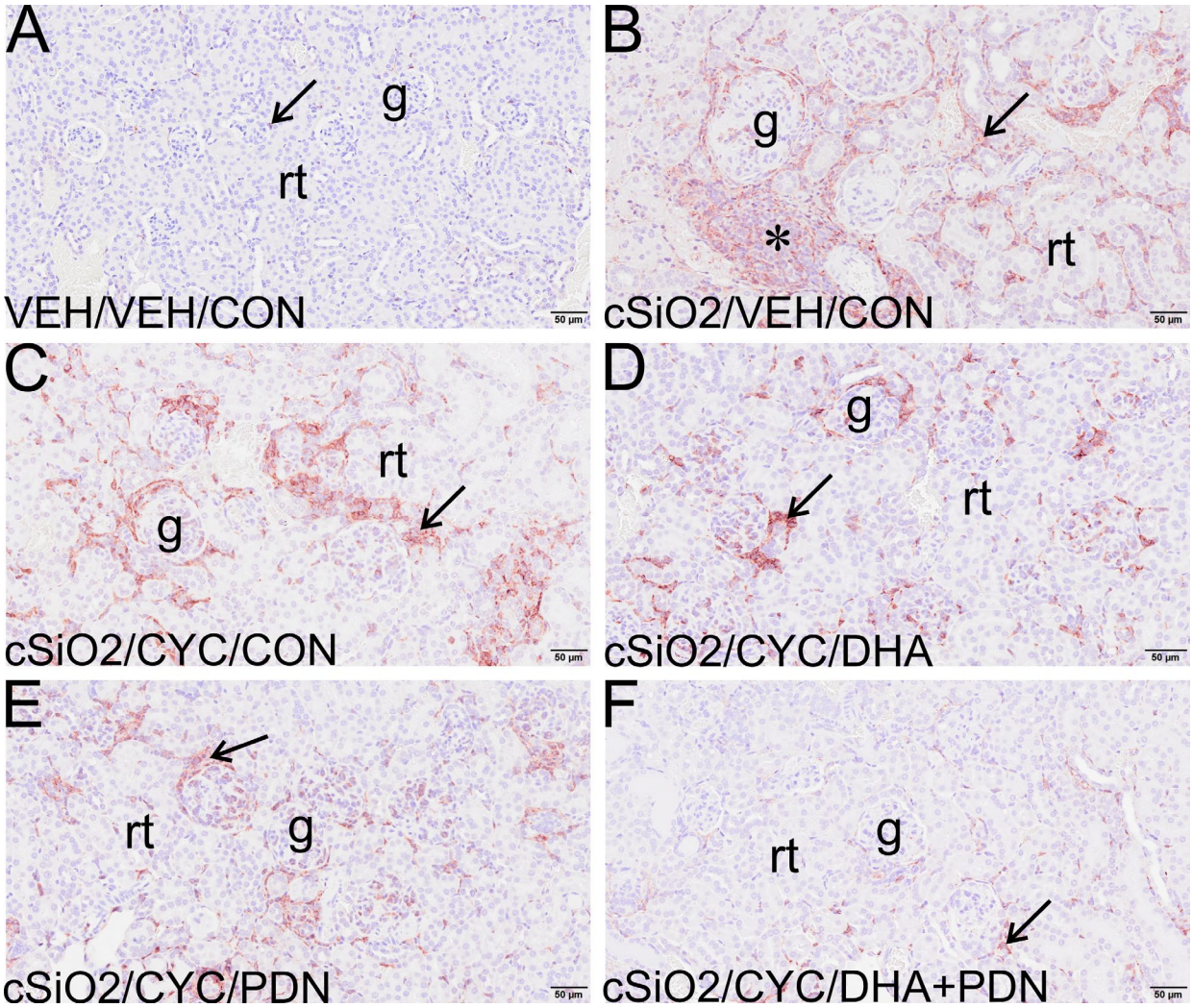
A
g
rt
VEH/VEH/CON
50 µm
B
g
*
rt
cSiO2/VEH/CON
50 µm
C
rt
g
cSiO2/CYC/CON
50 µm
D
g
rt
cSiO2/CYC/DHA
50 µm
E
rt
g
cSiO2/CYC/PDN
50 µm
F
rt
g
cSiO2/CYC/DHA+PDN
50 µm

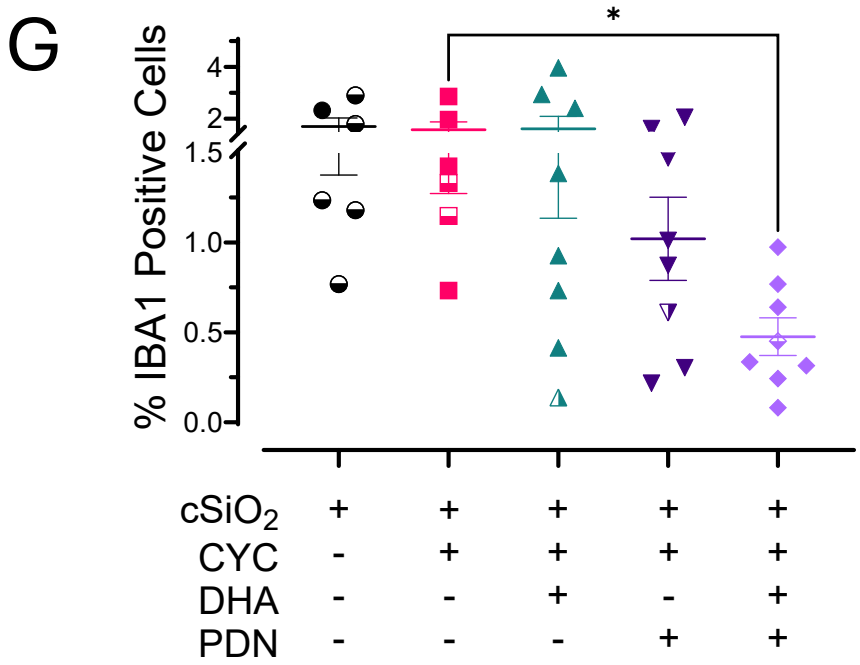
G
% IBA1 Positive Cells
4
2
1.5
1.0
0.5
0.0
*
cSiO2 + + + + +
CYC - + + + +
DHA - - + - +
PDN - - - + +

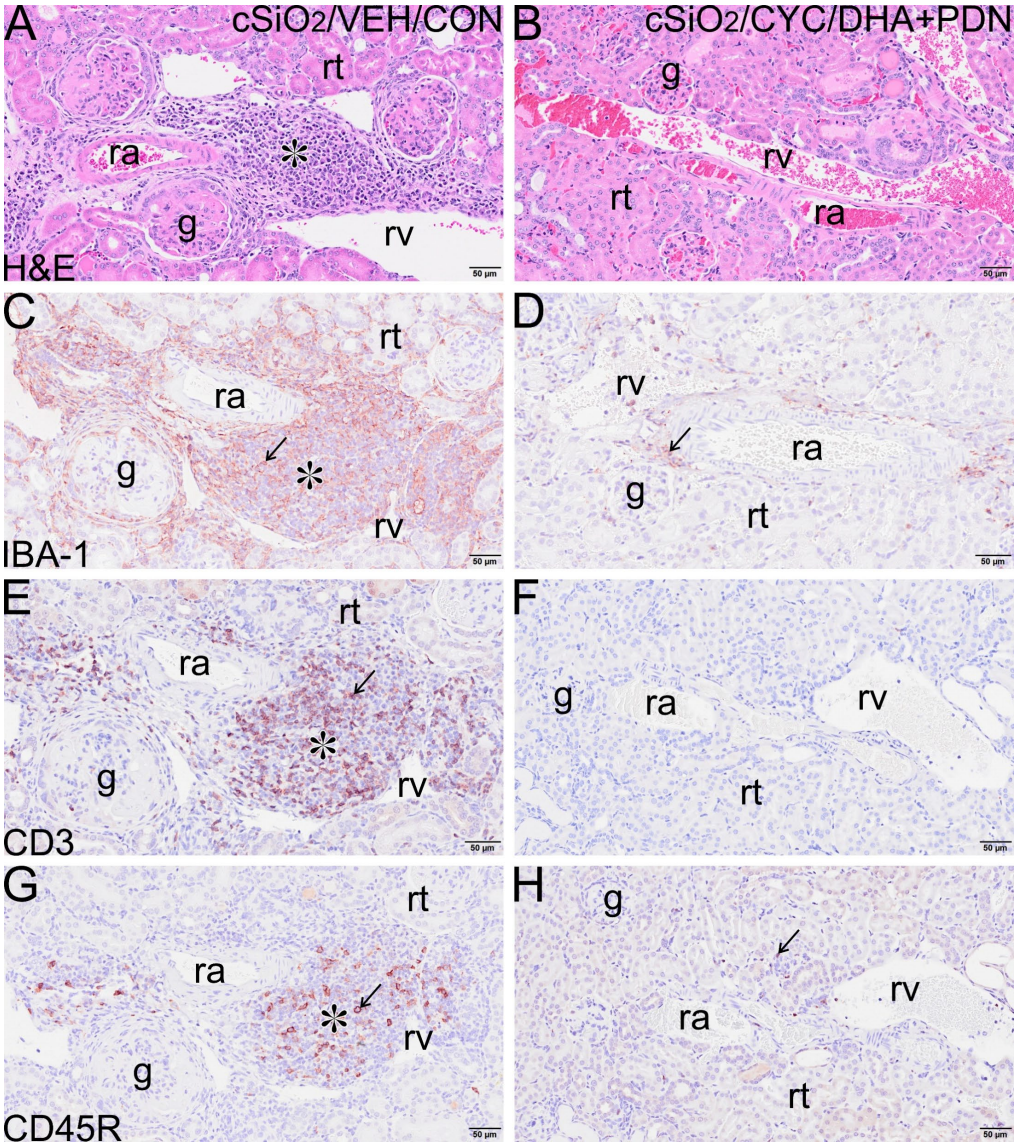
A
cSiO2/VEH/CON
rt
ra
g
rv
H&E
B
cSiO2/CYC/DHA+PDN
g
rv
rt
ra
C
rt
ra
g
rv
IBA-1
D
rv
ra
g
rt
E
rt
ra
g
rv
CD3
F
g
ra
rv
rt
G
rt
ra
rv
g
CD45R
H
g
rv
ra
rt

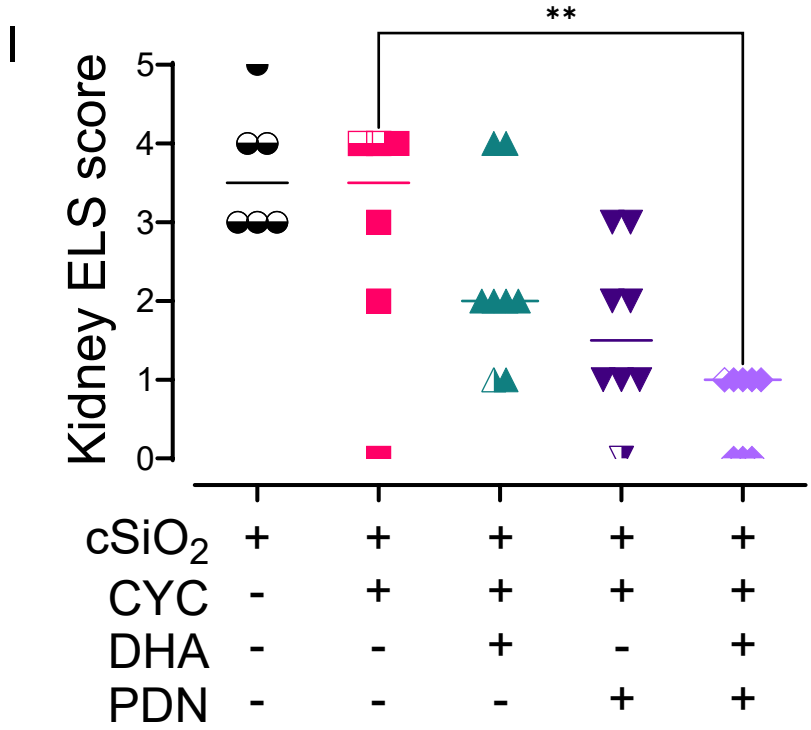
I
**
Kidney ELS score
5
4
3
2
1
0
cSiO2 + + + + +
CYC - + + + +
DHA - - + - +
PDN - - - + +

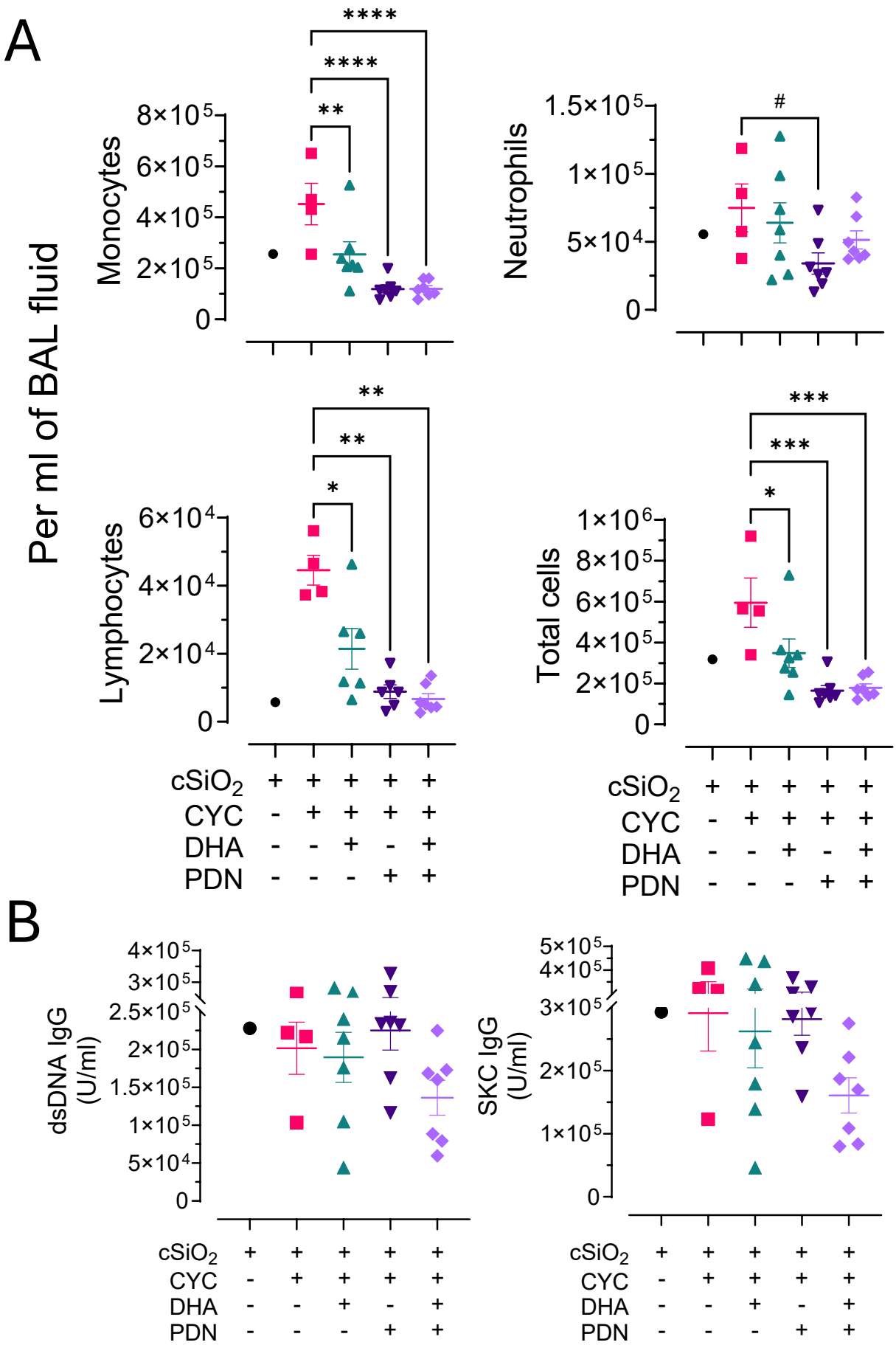
A
Per ml of BAL fluid
Monocytes
8×10^5
6×10^5
4×10^5
2×10^5
0
****
****
**
Neutrophils
1.5×10^5
1×10^5
5×10^4
0
#
Lymphocytes
6×10^4
4×10^4
2×10^4
0
**
**
*
Total cells
1×10^6
8×10^5
6×10^5
4×10^5
2×10^5
0
***
***
*
cSiO2 + + + + +
CYC - + + + +
DHA - - + - +
PDN - - - + +
B
dsDNA IgG (U/ml)
4×10^5
3×10^5
2.5×10^5
2×10^5
1.5×10^5
1×10^5
5×10^4
0
SKC IgG (U/ml)
5×10^5
4×10^5
3×10^5
2×10^5
1×10^5
0

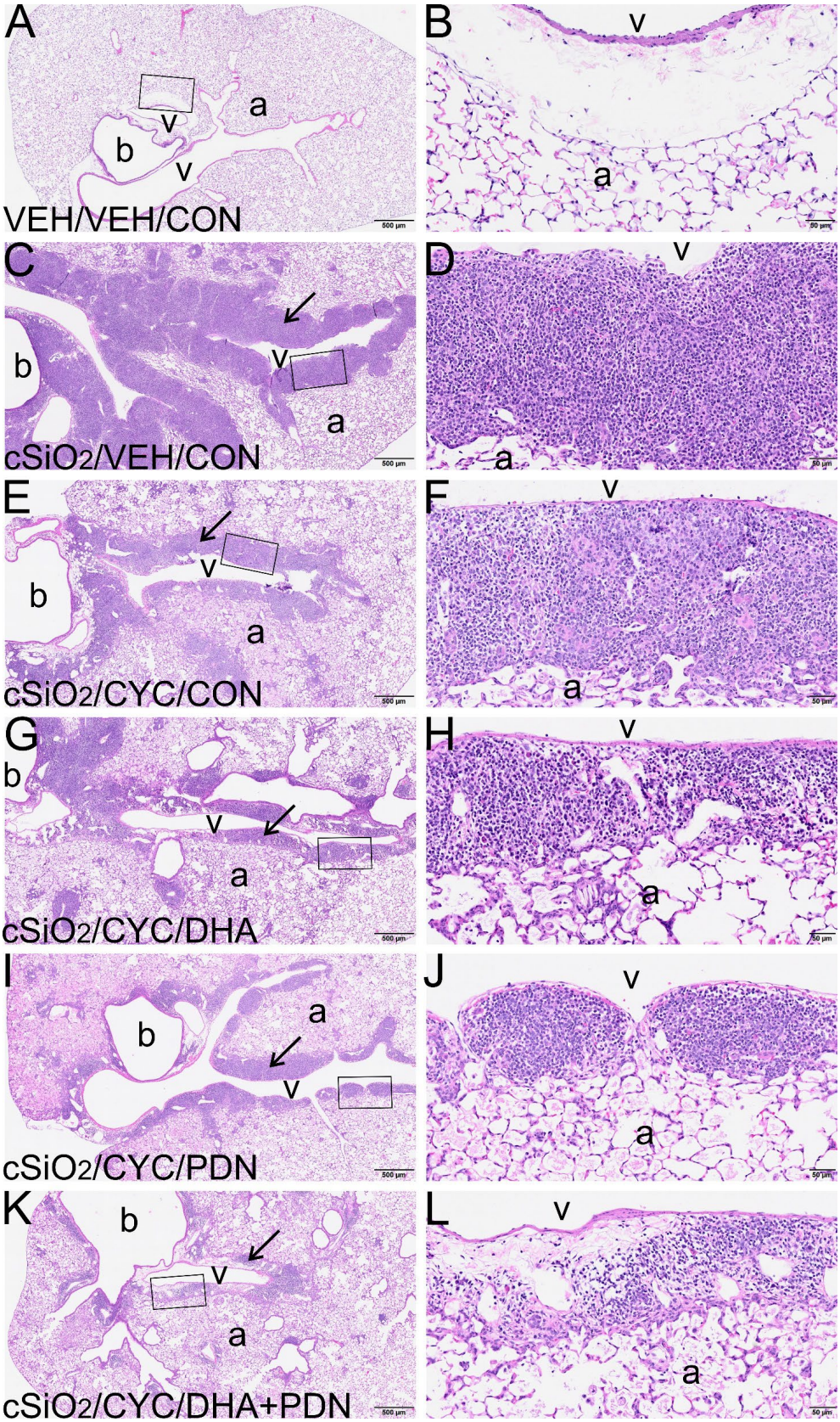
A
a
v
b
v
VEH/VEH/CON
B
v
a
C
b
v
a
cSiO2/VEH/CON
D
v
a
E
v
b
a
cSiO2/CYC/CON
F
v
a
G
b
v
a
cSiO2/CYC/DHA
H
v
a
I
b
a
v
cSiO2/CYC/PDN
J
v
a
K
b
v
a
cSiO2/CYC/DHA+PDN
L
v
a

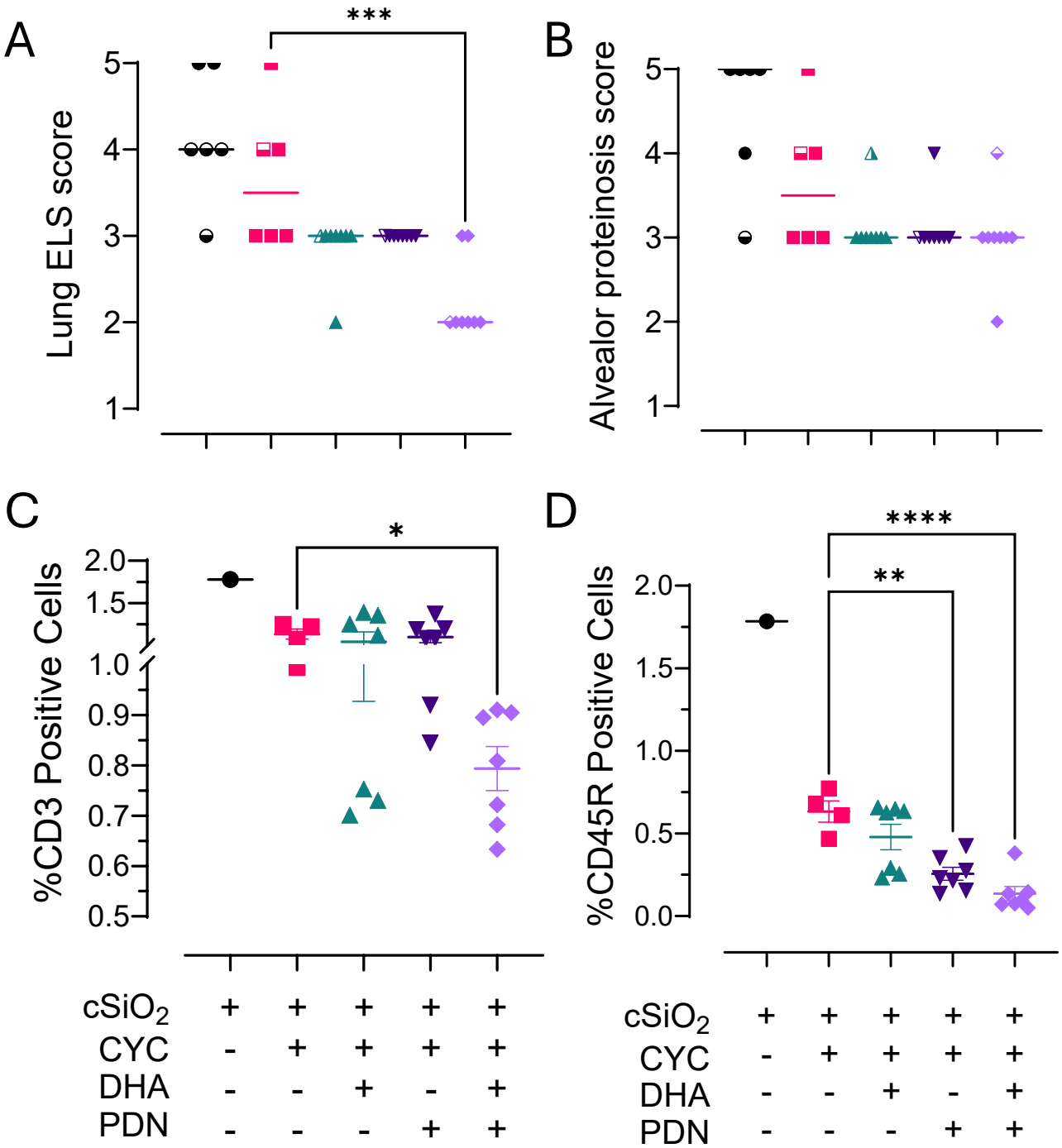
A
***
Lung ELS score
5
4
3
2
1
B
Alvealor proteinosis score
5
4
3
2
1
C
*
%CD3 Positive Cells
2.0
1.5
1.0
0.9
0.8
0.7
0.6
0.5
D
****
**
%CD45R Positive Cells
2.0
1.5
1.0
0.5
0.0
cSiO2 + + + + +
CYC - + + + +
DHA - - + - +
PDN - - - + +
cSiO2 + + + + +
CYC - + + + +
DHA - - + - +
PDN - - - + +

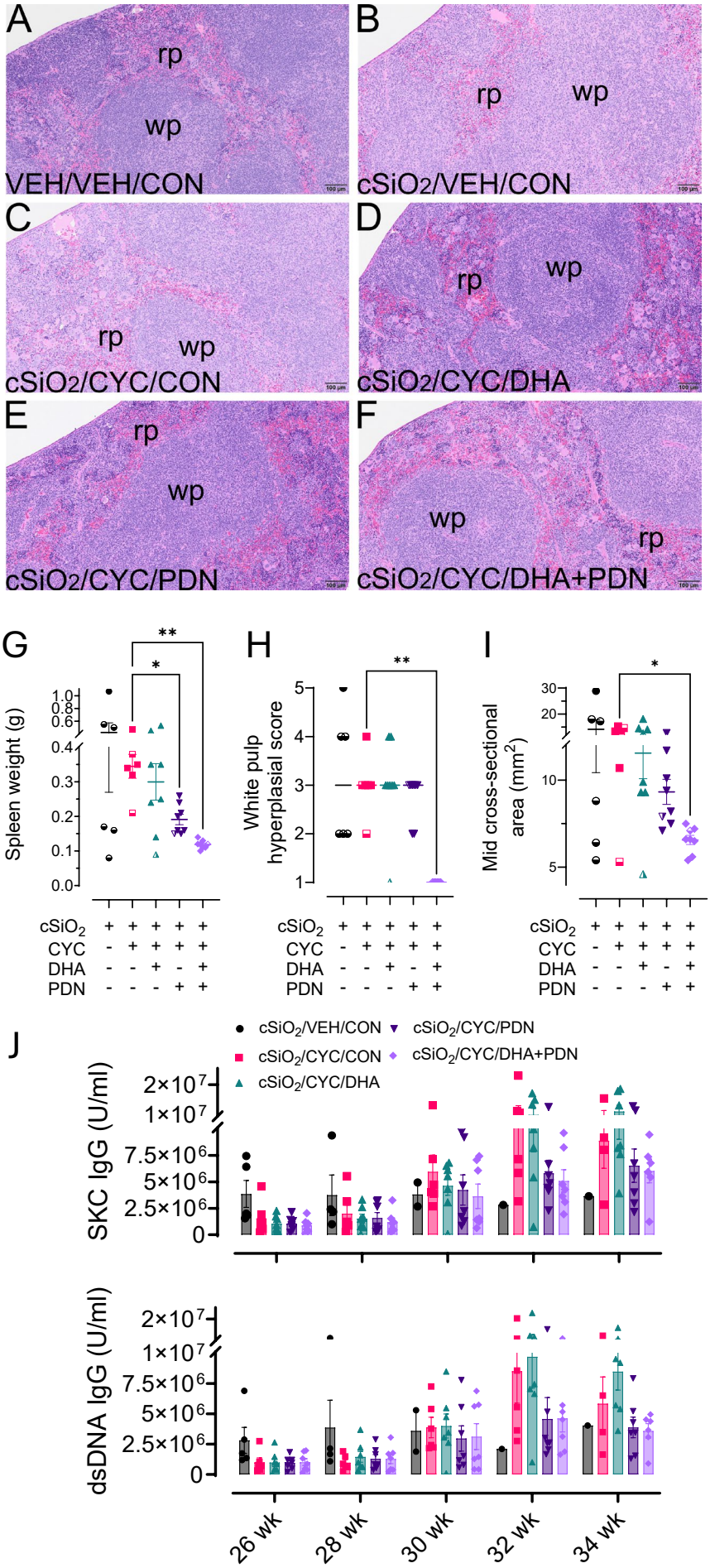
A
rp
wp
VEH/VEH/CON
B
rp
wp
cSiO2/VEH/CON
C
rp
wp
cSiO2/CYC/CON
D
rp
wp
cSiO2/CYC/DHA
E
rp
wp
cSiO2/CYC/PDN
F
wp
rp
cSiO2/CYC/DHA+PDN
G
Spleen weight (g)
H
White pulp hyperplasial score
I
Mid cross-sectional area (mm2)
cSiO2
CYC
DHA
PDN
J
cSiO2/VEH/CON
cSiO2/CYC/CON
cSiO2/CYC/DHA
cSiO2/CYC/PDN
cSiO2/CYC/DHA+PDN
SKC IgG (U/ml)
dsDNA IgG (U/ml)
26 wk
28 wk
30 wk
32 wk
34 wk

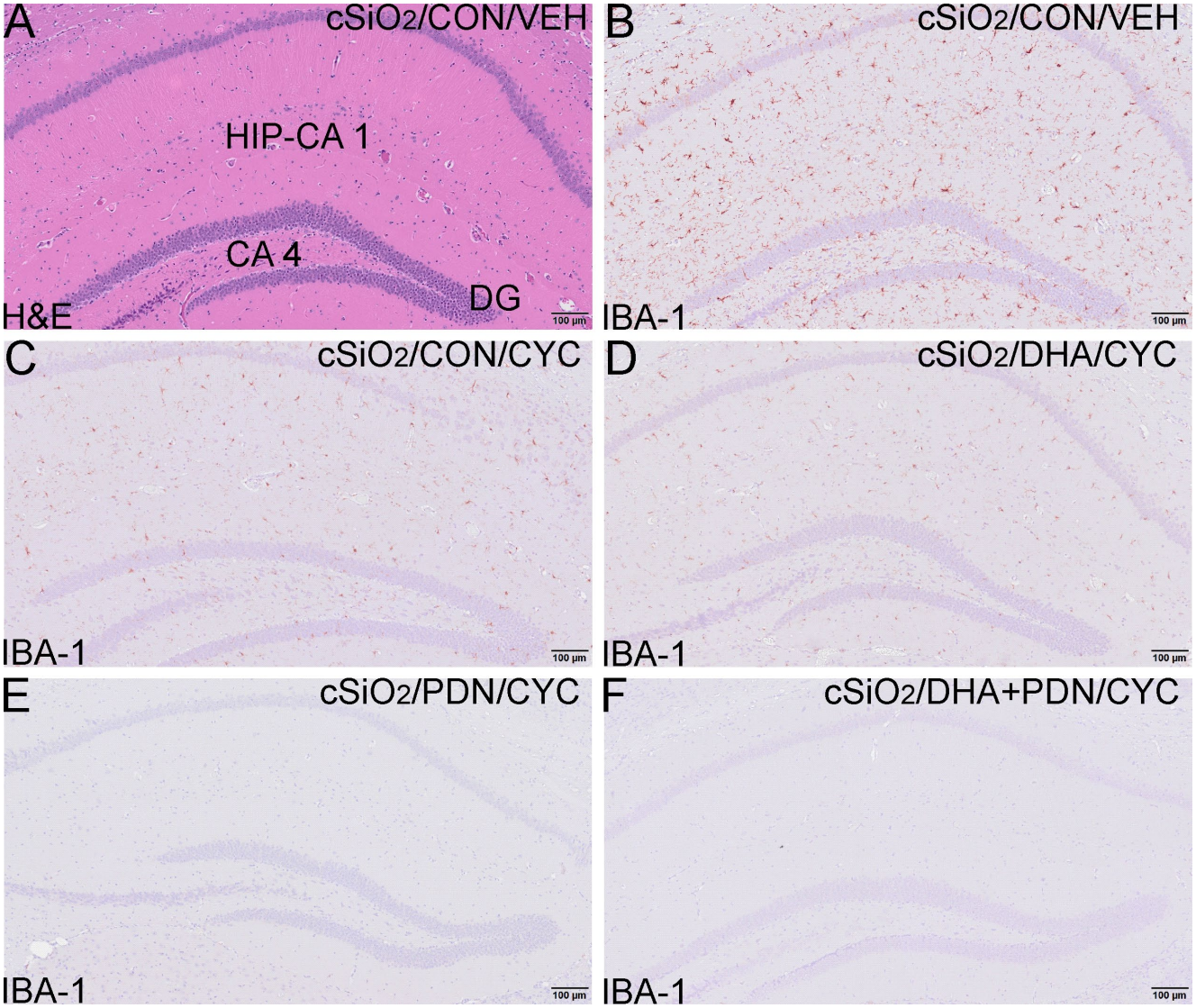
A
cSiO2/CON/VEH
HIP-CA 1
CA 4
DG
H&E
100 µm
B
cSiO2/CON/VEH
IBA-1
100 µm
C
cSiO2/CON/CYC
IBA-1
100 µm
D
cSiO2/DHA/CYC
IBA-1
100 µm
E
cSiO2/PDN/CYC
IBA-1
100 µm
F
cSiO2/DHA+PDN/CYC
IBA-1
100 µm

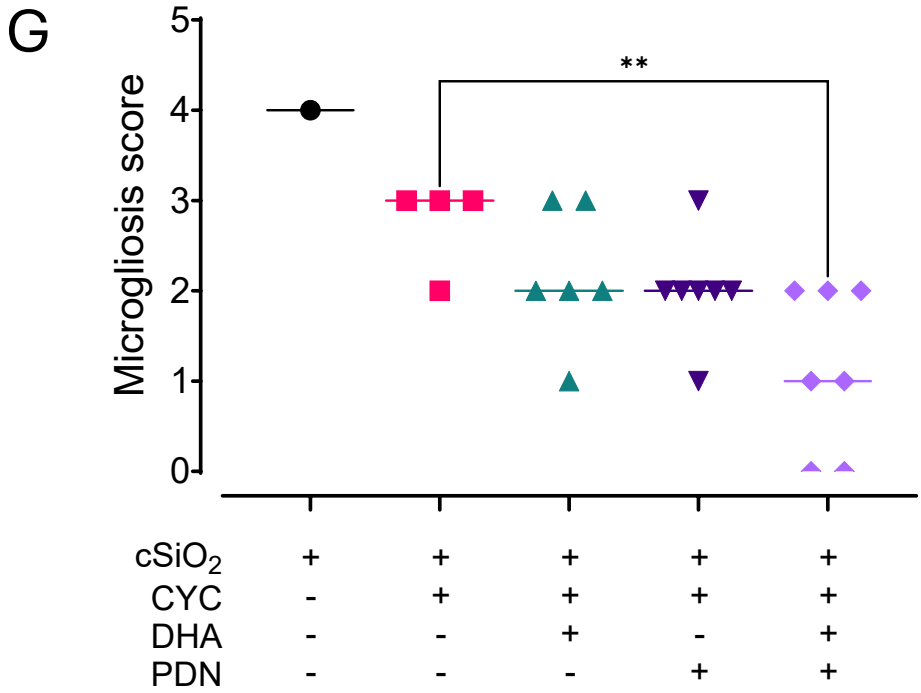
G
Microgliosis score
0
1
2
3
4
5
**
cSiO2 + + + + +
CYC - + + + +
DHA - - + - +
PDN - - - + +

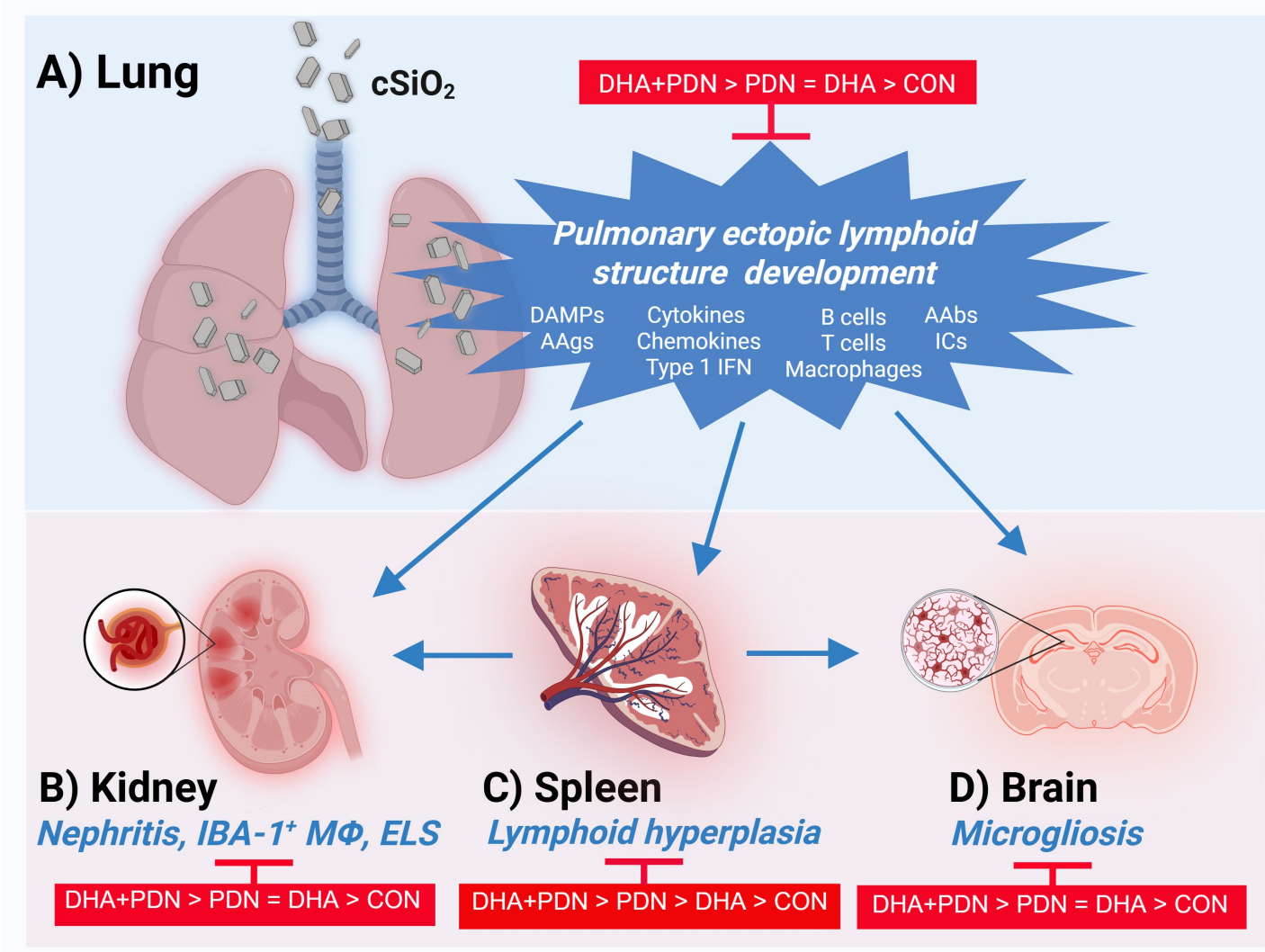
A) Lung
cSiO2
DHA+PDN > PDN = DHA > CON
Pulmonary ectopic lymphoid structure development
DAMPs
AAgs
Cytokines
Chemokines
Type 1 IFN
B cells
T cells
Macrophages
AAbs
ICs
B) Kidney
Nephritis, IBA-1+ MΦ, ELS
DHA+PDN > PDN = DHA > CON
C) Spleen
Lymphoid hyperplasia
DHA+PDN > PDN > DHA > CON
D) Brain
Microgliosis
DHA+PDN > PDN = DHA > CON

Reducing Glucocorticoid Burden in Lupus with Omega-3 Fatty Acids: Docosahexaenoic Acid Augments Prednisone Efficacy in Maintaining Cyclophosphamide-Induced Remission of Preclinical Lupus Nephritis

Ashley N. Anderson[1], Olivia F. McDonald[1,2], Shayla-Rae Johnson[1], John J. Liddle[1], Vanessa Estrada[1,2], Jalen T. Jackson[1], Ryan P. Lewandowski[3], James G. Wagner[2,3], Jack R, Harkema[2,3,4], James J. Pestka[1,2,5.]

[1] Department of Microbiology, Genetics, and Immunology, Michigan State University, East Lansing, MI, United States; [2] Institute for Integrative Toxicology, Michigan State University, East Lansing, MI, United States; [3] Department of Pathobiology and Diagnostic Investigation, Michigan State University, East Lansing, MI, United States; [4] Department of Pharmacology and Toxicology, Michigan State University, East Lansing, MI, United States; [5] Department of Food Science and Human Nutrition, Michigan State University, East Lansing, MI, United States

Supplemental Materials

- **Supplemental Methods:** Immunohistochemistry (IHC)
- **Supplementary Table 1.** List of key reagents, items, and kits
- **Supplementary Table 2.** Criteria for defining moribund condition of silica-treated NZBWF1 mice
- **Supplemental Figure 1**. Effects of DHA and PDN monotherapies and co-therapy on CYC-induced reduction of blood urea nitrogen (BUN) in the cSiO2-accelerated lupus nephritis mouse model

Supplemental Methods

Immunohistochemistry (IHC)

IHC was conducted as previously described (Pestka et al. 2021, Front. Immunol.12:653464). Briefly, formalin-fixed, paraffin-embedded samples were sectioned, placed on charged slides, and dried overnight at 56°C. The slides were then deparaffinized in xylene and rehydrated through using a dilution series of ethanol ending with distilled water. . Slides were immersed in tris-buffered saline pH 7.4 (TBS, Scytek Labs, Logan, UT) for 5 minutes to adjust the pH. Following TBS, retrieval protocols were applied according to the requirements of each primary antibody. Endogenous peroxidase activity was blocked for 30 minutes at room temperature in a solution of 3% hydrogen peroxide in methanol (1:4), then rinsed with running tap water, followed by several rinses in distilled water, and a 5-minute incubation in TBS containing Tween 20 (Scytek Labs, Logan, UT). After pretreatment, standard micropolymer complex staining steps were performed at room temperature using the Biocare Medical intelliPATH FLX automated IHC staining instrument. Rinses after each staining step were carried out with TBS autowash buffer containing surfactant (TWB945M, Biocare Medical, Pacheco, CA).

After blocking for nonspecific protein with rodent block M (Biocare Medical, Pacheco, CA) or IntelliPATH background punisher (IP974G20, Biocare Medical, Pacheco, CA) for 20 or 5 minutes, respectively, tissue sections were incubated with primary antibodies (anti-IBA1 1:3000, anti-CD3 1:200, anti-CD45R 1:250) in normal antibody diluent (Scytek Labs, Logan, UT). MicroPolymer Rabbit on Rodent HRP Polymer was used for the CD3 and IBA1 primary antibodies, and Rat on Mouse HRP Probe & Polymer for the CD45R primary antibody. To visualize the target proteins, the substrate Biocare Medical Romulin AEC Chromogen was incubated with the tissue for 5 minutes, then counterstained with CATHE Hematoxylin (Biocare Medical, Pacheco, CA) at a dilution of 1:10 for 1 minute. Afterwards, slides were air-dried, cleared, and mounted with synthetic mounting media.

Supplementary Table 1. List of key reagents, items, and kits.

Reagent, item, or kit	Vendor	Catalog Number
AIN-93G Purified Rodent Diet without Vitamin Mix	Dyets Inc.	110700
AIN-93G VX Vitamin Mix	Dyets Inc.	310025
LouAna Safflower Oil	LouAna Oils	
AVO high-oleic safflower oil	American Vegetable Oils, Inc.	
Mazola Corn Oil	Mazola	
Cyclophosphamide	Sigma-Aldrich	C0768-1G
Prednisone	Spectrum Chemical Mfg. Corp.	PR103-25GM
DHASCO, Microalgal Oil Containing 40% DHA	DSM Nutritional Products	
Crystalline Silica	U.S. Silica	Min-U-Sil-5
Polyclonal Rabbit Anti – Iba1Antibody	Wako Fuji	019-19741
Polyclonal Rabbit anti – CD3	Abcam	Ab5690
Monoclonal Rat anti – Mouse CD45R	BD Pharmingen	550286
Uristix 4	Siemens Healthineers	
CLINITEK Status+ Urine Analyzer	Siemens Healthineers	
Urea Nitrogen (BUN) Detection Assay Kit (Colorimetric)	RayBiotech	MA-BUN-5
Polyclonal Rabbit Anti-Mouse CD3 Antibody	Abcam	ab5690
Monoclonal Rat Anti-Mouse CD45R Antibody	Becton Dickinson	550286
Mouse Cytokine/Chemokine 44-Plex Discovery Assay® Array	Eve Technologies	MD44
Nunc 96-Well Flat Bottom MaxiSorp Immuno Plates	Thermo Fisher Scientific	442404
Corning® Phosphate-Buffered Saline, 1X without calcium and magnesium, PH 7.4 ± 0.1	Corning	21-040-CV
HyClone DPBS 10X without calcium, magnesium	Cytiva	SH30378.03
Poly-L-Lysine Solution, 0.1% (w/v)	Sigma Aldrich	P8920
Purified Native dsDNA, Calf Thymus	Alpha Diagnostic International	DNAD25-N-1
Anti-DNA Antibody, double stranded, clone BV16-13	Millipore Sigma	MAB030
Goat Anti-Mouse IgG (heavy-chain sp.)-HRP conjugate	Alpha Diagnostic International	40120
K-Blue® Advanced TMB Substrate	Neogen	319176

Supplementary Table 2. Criteria for defining moribund condition of silica-treated NZBWF1 mice[a]

Criteria	Method	Response	Score Assigned
Proteinuria[1,2]	Weekly monitoring	<2000 mg/dl = negative (NEG)	0
		>2000 mg/dl = positive (POS)	1
	Note: proteinuria scoring is cumulative over time		
	e.g., POS for proteinuria at 22 wks of age and POS at 23 wks of age = cumulative score of 2		
Weight Loss[2,3,4,5]	Weekly body weight	<10% loss = NEG	0
		10-14% loss = POS	2
		>15% loss = POS	4
	Note #1: loss of body weight will be calculated relative to body weight at onset of nephritis		
	Note #2: onset of nephritis defined as = 300 mg/dl proteinuria (determined in above measurements)		
Dyspenia[1,3,4,5,*]	Daily health check	Qualitative - NO	0
		Qualitative - YES	1
Ambulation[3,4,5,*]	Daily health check	Qualitative - NO	0
		Qualitative - YES	4
Rough Coat[3,4,5,*]	Daily health check	Qualitative - NO	0
		Qualitative - YES	1

[a] Table was reviewed by CAR Veterinarian Dr. Danielle Ferguson at Michigan State University. Mice receiving a score of 4 or more were euthanized. References for criteria previously published indicated by superscripts and noted below.

[1]Gardet et al. (2016) PLOS ONE. 11(10): e 0164423
[2]Frese-Schaper et al. (2010) J Immunology 184 (4) 2175-2182
[3]Toth, L. (2000). Journal of the Institute for Laboratory Animal Research (2000) 41 (2): 72-29
[4]Toth, L. (1997). Contemp. Top Lab Anim Sci 36, 44-48
[5]Tomasovic et al. (1988). Lab Animal 17:31-34,1998.
*The IACUC Handbook (2014) CRC Press. 3rd Edition

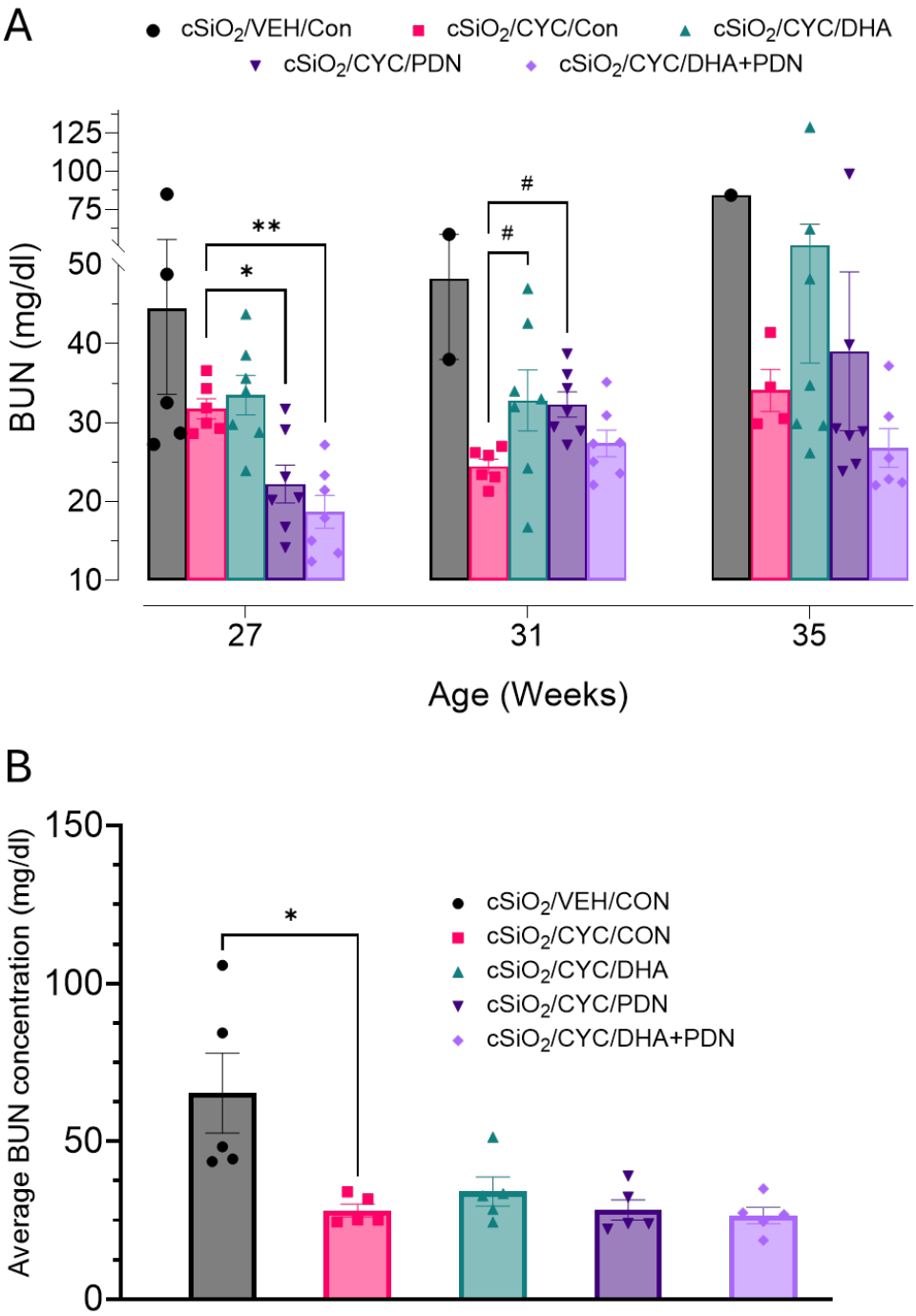

Supplemental Figure 1. Effects of DHA and PDN monotherapies and co-therapy on CYC-induced reduction of blood urea nitrogen (BUN) in the $cSiO_2$-accelerated lupus nephritis mouse model. (A) BUN values at specific time points during the study. (B) Average BUN levels from weeks 27-35 of the study. Symbols: #, * , and ** denote significant differences at the $p<0.1$, $p<0.05$, and $p<0.01$ levels, respectively.